2004-06

An investigation of a multiple-input-multiple-output communication system with the Alamouti Space-time code

Turpin, Michael J.

Monterey, California. Naval Postgraduate School

NAVAL POSTGRADUATE SCHOOL

MONTEREY, CALIFORNIA

THESIS

AN INVESTIGATION OF A MULTIPLE–INPUT–MULTIPLE–OUTPUT COMMUNICATION SYSTEM WITH THE ALAMOUTI SPACE–TIME CODE

by

Michael J. Turpin

June 2004

Thesis Advisor: Frank Kragh

Approved for public release; distribution unlimited

THIS PAGE INTENTIONALLY LEFT BLANK

REPORT DOCUMENTATION PAGE			Form Approved OMB No. 0704-0188
Public reporting burden for this collection of information is estimated to average 1 hour per response, including the time for reviewing instruction, searching existing data sources, gathering and maintaining the data needed, and completing and reviewing the collection of information. Send comments regarding this burden estimate or any other aspect of this collection of information, including suggestions for reducing this burden, to Washington headquarters Services, Directorate for Information Operations and Reports, 1215 Jefferson Davis Highway, Suite 1204, Arlington, VA 22202-4302, and to the Office of Management and Budget, Paperwork Reduction Project (0704-0188) Washington DC 20503.			
1. AGENCY USE ONLY ***(Leave blank)***	**2. REPORT DATE** June 2004	**3. REPORT TYPE AND DATES COVERED** Master's Thesis	
4. TITLE AND SUBTITLE: An Investigation of a Multiple–Input–Multiple–Output Communication System with the Alamouti Space–Time Code			**5. FUNDING NUMBERS**
6. AUTHOR(S) Michael Turpin			
7. PERFORMING ORGANIZATION NAME(S) AND ADDRESS(ES) Naval Postgraduate School Monterey, CA 93943-5000			**8. PERFORMING ORGANIZATION REPORT NUMBER**
9. SPONSORING /MONITORING AGENCY NAME(S) AND ADDRESS(ES) N/A			**10. SPONSORING/MONITORING AGENCY REPORT NUMBER**
11. SUPPLEMENTARY NOTES The views expressed in this thesis are those of the author and do not reflect the official policy or position of the Department of Defense or the U.S. Government.			
12a. DISTRIBUTION / AVAILABILITY STATEMENT Approved for public release; distribution is unlimited			**12b. DISTRIBUTION CODE**
13. ABSTRACT (maximum 200 words) This thesis investigates the fundamentals of Multiple–Input–Multiple–Output (MIMO) radio communication systems with space–time codes. A MIMO system was design using the Alamouti space–time code. The modulation technique was binary phase-shift keying (BPSK). Matlab with Simulink was used to simulate the design, which was tested in both an additive white Gaussian noise (AWGN) channel and in a multipath fading channel with AWGN. Theoretical performance was derived for both channels and compared to simulated results. The original receiver design was changed to incorporate a maximal-ratio combiner (MRC) receiving technique with channel state information (CSI). The theoretical performance for this design was determined and compared to simulated and published results.			
14. SUBJECT TERMS Multiple–Input–Multiple–Output, Alamouti Scheme, Space–Time Coding, Binary Phase-Shift Keying, Rayleigh Fading Channel, Multipath fading channel, Maximal-Ratio Combining, Spectral efficiency, Channel Capacity, MIMO, BPSK, MRC			**15. NUMBER OF PAGES** 113
			16. PRICE CODE
17. SECURITY CLASSIFICATION OF REPORT Unclassified	**18. SECURITY CLASSIFICATION OF THIS PAGE** Unclassified	**19. SECURITY CLASSIFICATION OF ABSTRACT** Unclassified	**20. LIMITATION OF ABSTRACT** UL

NSN 7540-01-280-5500 Standard Form 298 (Rev. 2-89)
Prescribed by ANSI Std. 239-18

THIS PAGE INTENTIONALLY LEFT BLANK

Approved for public release; distribution unlimited

AN INVESTIGATION OF A MULTIPLE–INPUT–MULTIPLE–OUTPUT OMMUNICATION SYSTEM WITH THE ALAMOUTI SPACE–TIME CODE

Michael J. Turpin
Lieutenant Commander, Canadian Navy
B.S., University of Ottawa, 1984

Submitted in partial fulfillment of the
requirements for the degree of

MASTER OF SCIENCE IN ELECTRICAL ENGINEERING

from the

NAVAL POSTGRADUATE SCHOOL
June 2004

Author: Michael Turpin

Approved by: Frank Kragh
Thesis Advisor

Clark Robertson
Second Reader

John P. Powers
Chairman, Department of Electrical and Computer Engineering

THIS PAGE INTENTIONALLY LEFT BLANK

ABSTRACT

This thesis investigates the fundamentals of multiple–input–multiple–output (MIMO) radio communication systems with space–time codes. A MIMO system was designed using the Alamouti space–time code. The modulation technique was binary phase-shift keying (BPSK). Matlab with Simulink was used to simulate the design, which was tested in both an additive white Gaussian noise (AWGN) channel and in a multipath fading channel with AWGN. Theoretical performance was derived for both channels and compared to simulated results. The original receiver design was changed to incorporate a maximal-ratio combiner (MRC) receiving technique with channel state information (CSI). The theoretical performance for this design was determined and compared to simulated and published results.

THIS PAGE INTENTIONALLY LEFT BLANK

TABLE OF CONTENTS

LIST OF FIGURES

THIS PAGE INTENTIONALLY LEFT BLANK

LIST OF TABLES

THIS PAGE INTENTIONALLY LEFT BLANK

ACKNOWLEDGMENTS

I thank my incredible wife Cheryl for the sacrifice, love and support that she has made during the course of my studies at NPS. I also thank her for bringing our son Noah into our lives. For both of them, I am eternally grateful.

I would like to thank my advisor Frank Kragh for his patience and guidance. Without his help this thesis would not have been possible. I hope that this thesis helps his research in some way.

THIS PAGE INTENTIONALLY LEFT BLANK

EXECUTIVE SUMMARY

In modern radio communications, the demand for high speed, reliable communication together with efficient use of the spectrum and power are the prime technical criteria for communications engineers. However, these implementations must operate in a severe environment. They must confront rich scattering effects and multipath propagation under limited power constraints. This not only restricts the speed of communications but the reliability as well. Multiple–input–multiple–output (MIMO) communication systems with space–time coding provide increased reliability and increased capacity without bandwidth expansion. MIMO communications systems have application to existing and future military radio communications systems where channel bandwidth is restricted but increased capacity is necessary. If the information rate needs to double and must fit within the existing bandwidth, then MIMO communications systems can provide the increase in capacity.

This thesis investigated the fundamentals of MIMO systems with space–time coding. A simulation of a simple design was created to demonstrate and analyze performance. The space–time code chosen was the Alamouti scheme using binary phase–shift keying (BPSK) with a two transmit and two receive antenna MIMO system. The system design was implemented in Matlab with Simulink. The design was tested in an additive white Gaussian noise (AWGN) channel and then a multipath fading channel with AWGN. The original design was modified using a maximal-ratio combiner (MRC) technique and tested in a multipath channel with AWGN. The simulated performance results are compared with theoretical analysis as well as published results.

The results showed that the designed MIMO system performed within expectation of theoretical analysis in AWGN. It outperformed a single-channel BPSK system, needing 3.0 dB less power for equal performance. However, the designed system failed in a multipath channel. The MRC design was incorporated in the receiver. As a result, the new design was able to communicate successfully over the multipath channel. The performance of the new design matched expected theoretical performance as well as published results. The designed MIMO system with the MRC receiver was able to achieve

full diversity order with the Alamouti space–time code which was consistent with published results. It was able to achieve a significant advantage over a single-channel BPSK, or single–input–single–output (SISO) system, in a multipath channel with AWGN.

I. INTRODUCTION

A. BACKGROUND

In modern radio communications the demand for high speed, reliable communication together with efficient use of the spectrum and power are the prime technical criteria for communications engineers. For example, the implementation of wireless Internet with video conferencing or other media applications requires wideband, high data rate and reliable communication systems. However, these implementations must operate in a severe environment. They must confront rich scattering effects and multipath propagation under limited power constraints. This not only restricts the speed of communications, but the reliability as well. Added to this is the limited available spectrum that is allocated for wireless systems. Limited bandwidth means limited data rates, or speed of communications. What if a system can be implemented that provides reliability and increased capacity within limited bandwidth constraints? This would give the communications engineer more avenues for trade-offs in design. The demand for increased capacity within limited bandwidths is certainly relevant to existing and future military communications systems. A multiple–input–multiple–output (MIMO) communication system with space–time coding holds such a promise for engineers. "Recent research in information theory has shown that large gains in capacity of communication over wireless channels are feasible in multiple–input–multiple–output systems."[1] A review of MIMO related literature finds the quote or variations of it several times. The primary focus of this research was to investigate the fundamentals of MIMO systems.

B. GOALS AND METHODOLOGY

The goal of this thesis was to examine MIMO systems with space–time coding and their relevance to military communication systems. In order to do so, a simulation of a simple system was created to demonstrate and analyze the design's performance. The space–time code chosen here is the Alamouti scheme using binary phase–shift keying (BPSK) with a two transmit antenna and two receive antenna MIMO system [1]. The modulator and simple receiver design were created and implemented in Matlab with Simulink. The design was realized in equivalent baseband form to facilitate comparison

with published theory. The design was tested first in additive white Gaussian noise (AWGN). Theoretical performance was determined and compared with simulated results of a single channel BPSK system, or single–input–single–output (SISO) system. The design was then progressed to a multipath fading channel with AWGN. The simulated performance results were compared with theoretical results as well as published results.

C. BENEFITS OF STUDY

Space–time coding in MIMO systems is new technology. There is a great deal of research effort in this technology [1]. The demand for high speed reliable communications systems in a limited frequency spectrum for commercial use is mimicked by military applications. However, some military applications also need capacity and concealment. If increased capacity and performance at a certain power level is achieved, then the power level may be reduced by sacrificing capacity. Nevertheless, this may be at a capacity that is already acceptable. The reduced power level may lead into a region of low probability of detection communications and concealment. Notwithstanding, MIMO and space–time coding holds promise for additional trade-offs for the communications engineer.

D. THESIS ORGANIZATION

This thesis is organized in four remaining chapters. Chapter II introduces the fundamentals of the MIMO model. It discusses capacity, the channel and the significant aspects of MIMO and space–time coding. Chapter III introduces the design of the MIMO communications system using the Alamouti space–time code [1]. The transmitter, receiver and logic of the receiver's creation will be discussed. Examination of the theoretical and simulated performance of the MIMO system design is detailed in Chapter IV. It progresses through performance in AWGN to performance in a multipath fading channel with AWGN. Chapter V reviews the results and concludes with recommendations for future study. Additionally, there are two appendices: Appendix A is a list the acronyms, and Appendix B contains the block parameters used in the simulations.

II. MULTIPLE–INPUT–MULTIPLE–OUTPUT

This chapter lays the groundwork for understanding and analyzing MIMO systems in a multipath fading environment. The MIMO model is introduced and the MIMO capacity equation is derived. The capacity of a MIMO system is greater than that of a SISO system [2]. The increase in capacity of MIMO systems is the driving force of much of the research in this area. Next, an overview of the multipath fading channel is presented. The signal will be subjected to multipath fading, so a baseband model is described to facilitate analysis. Then, diversity techniques and the maximal-ratio combiner (MRC) are described. A firm understanding is necessary for analysis of the performance of the design. Finally, space–time codes are introduced. Space–time coding is a mechanism to approach the capacity of a MIMO system [1]. The analysis in this thesis is performed in the baseband transmission model. Thus, a definition of the baseband transmission model is introduced first. This chapter provides the fundamentals needed to analyze the design of the MIMO system with the Alamouti scheme.

A. BASEBAND TRANSMISSION MODEL

The baseband transmission model is the lowpass equivalent of the bandpass transmission model [3]. It consists of the complex lowpass representation or baseband equivalents of bandpass signals and the bandpass channel transfer function as illustrated in Figure 1. In Figure 1, the input bandpass signal is represented by $x(t)$ and its Fourier transform $X(f)$. The bandpass system's impulse response is represented by $h(t)$ and its Fourier transform $H(f)$. Lastly, the output of the system is represented by $y(t)$ and its Fourier transform $Y(f)$. Let the baseband equivalent of each of the signals and transfer function be distinguished by a tilde, i.e., $\tilde{x}(t)$, $\tilde{h}(t)$ and $\tilde{y}(t)$. Similarly, the Fourier transforms of the baseband equivalent system are represented by $\tilde{X}(f)$, $\tilde{H}(f)$ and $\tilde{Y}(f)$.

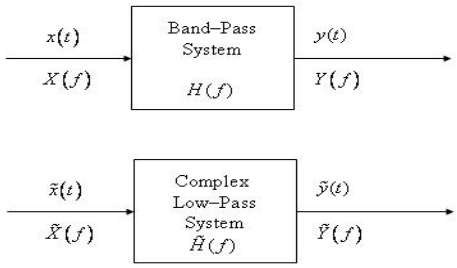

Figure 1. Bandpass and equivalent lowpass system (After Reference [3].).

The input signal $x(t)$ is related to its baseband equivalent by [3]

$$x(t) = \mathrm{Re}\left[\tilde{x}(t)e^{j2\pi f_c t}\right], \tag{2.1}$$

where $\mathrm{Re}[\ ]$ represents the real part of the expression in the brackets and f_c is the carrier frequency of the bandpass system. The baseband equivalent signal $\tilde{x}(t)$ can be represented by its inphase and quadrature components $x_I(t)$ and $x_Q(t)$ by [3]

$$\tilde{x}(t) = x_I(t) + jx_Q(t), \tag{2.2}$$

where

$$x_I(t) = \mathrm{Re}\left[\tilde{x}(t)\right], \tag{2.3}$$

and

$$x_Q(t) = \mathrm{Im}\left[\tilde{x}(t)\right]. \tag{2.4}$$

The $\mathrm{Im}[\ ]$ is the imaginary part of the function inside the brackets.

The magnitude of the frequency response of the bandpass system $H(f)$ and that of the complex lowpass equivalent system $\tilde{H}(f)$ are illustrated in Figure 2. The baseband equivalent transfer function $\tilde{H}(f)$ can be obtained by shifting the positive fre-

quency components of the bandpass transfer function $H(f)$ by f_c to be centered about zero [3]. The transfer function is assumed to flat over the bandwidth B.

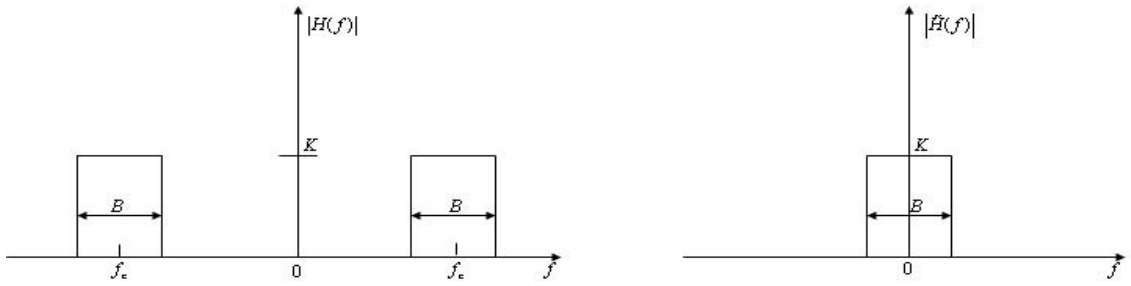

Figure 2. Bandpass and equivalent lowpass transfer function (After Reference [3].).

From Figure 1, the Fourier transform of the output signal of the bandpass system $Y(f)$ and baseband equivalent system is given by [3]

$$Y(f) = X(f)H(f). \tag{2.5}$$

The baseband equivalent is given by

$$\tilde{Y}(f) = \tilde{X}(f)\tilde{H}(f). \tag{2.6}$$

It is assumed that the bandwidth of $\tilde{x}(t)$ is small enough such that the magnitude and phase of $\tilde{H}(f)$ can be considered constant in this bandwidth of interest; specifically,

$$H(f) = he^{j\varphi}, \tag{2.7}$$

where h is a positive real number and φ is in the range of $[0, 2\pi]$. Then $\tilde{h}(t)$ is given by

$$\tilde{h}(t) = he^{j\varphi}\delta(t). \tag{2.8}$$

where $\delta(t)$ is the Dirac delta function. The baseband equivalent output signal $\tilde{y}(t)$ is the convolution of $\tilde{x}(t)$ and $\tilde{h}(t)$, given by

$$\begin{aligned}\tilde{y}(t) &= \int_{-\infty}^{\infty} \tilde{x}(\tau)\tilde{h}(t-\tau)d\tau \\ &= \int_{-\infty}^{\infty} \tilde{x}(\tau) h e^{j\varphi}\delta(t-\tau)d\tau \\ &= \tilde{x}(t) h e^{j\varphi}.\end{aligned} \tag{2.9}$$

The bandpass output signal $y(t)$ is related to the its complex equivalent $\tilde{y}(t)$ by [3]

$$y(t) = \mathrm{Re}\left[\tilde{y}(t)e^{j2\pi f_c t}\right]. \tag{2.10}$$

Like the input signal $\tilde{x}(t)$, the baseband equivalent output signal $\tilde{y}(t)$ can be decomposed into inphase and quadrature components by [3]

$$\tilde{y}(t) = y_I(t) + jy_Q(t), \tag{2.11}$$

where

$$y_I(t) = \mathrm{Re}\left[\tilde{y}(t)\right], \tag{2.12}$$

and

$$y_Q(t) = \mathrm{Im}\left[\tilde{y}(t)\right]. \tag{2.13}$$

The bandpass system can be obtained from its baseband equivalent. The information of contained in $x(t)$ and $y(t)$ are preserved in $\tilde{x}(t)$ and $\tilde{y}(t)$ [3]. In the rest of this thesis, the signals and systems are represented by their baseband equivalent.

B. THE MIMO MODEL

The MIMO model is described in Figure 3. The development of the model discussed in this section is largely based on Reference [1]. The model consists of N_t transmit and N_r receive antennas. From each transmit antenna, a signal x_j, where $j = 1, 2, 3, \ldots, N_t$, is transmitted. The signal x_j represents the baseband equivalent $\tilde{x}_j(t)$.

(The function of t has been dropped for convenience.) Each signal x_j passes through N_r channels represented by h_{ij}. It is assumed that the bandwidth of the signals x_j is small enough that Equation (2.9) holds true. The symbol h_{ij} is a complex number given by

$$h_{ij} = \left|h_{ij}\right| e^{j\varphi_{ij}}, \tag{2.14}$$

and will be referred to as the channel coefficients. At each receive antenna, white Gaussian noise (AWGN) n_i, where $i = 1, 2, 3, \ldots, N_r$, is added to the signal. The symbol n_i represents the AWGN baseband equivalent $\tilde{n}_i(t)$ [1]. The received signal is represented as r_i, where $i = 1, 2, 3, \ldots, N_r$, and is the baseband equivalent of the received signal $\tilde{r}_i(t)$.

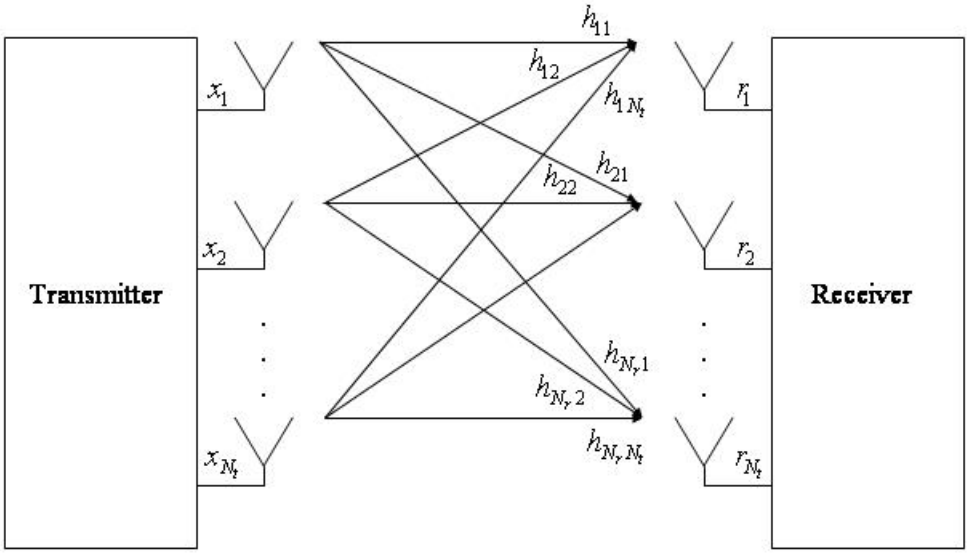

Figure 3. MIMO model (After Reference [1].).

At any receive antenna i, the received signal r_i is the sum of the transmitted signals through the channel and the AWGN and is given by [1]

$$
\begin{aligned}
r_i &= h_{i1}x_1 + h_{i2}x_2 + \ldots + h_{iN_t}x_{N_t} + n_i \\
&= \begin{bmatrix} h_{i1} & h_{i2} \cdots h_{iN_t} \end{bmatrix} \begin{bmatrix} x_1 \\ x_2 \\ \vdots \\ x_{N_t} \end{bmatrix} + n_i .
\end{aligned} \tag{2.15}
$$

Thus, the system as a whole can be represented as a system of linear equations given by [1]

$$
\begin{bmatrix} r_1 \\ r_2 \\ \vdots \\ r_{N_r} \end{bmatrix} = \begin{bmatrix} h_{11} & h_{12} \cdots h_{1N_t} \\ h_{21} & h_{22} \cdots h_{2N_t} \\ \vdots & \vdots \quad \vdots \\ h_{N_r1} & h_{N_r2} \cdots h_{N_rN_t} \end{bmatrix} \begin{bmatrix} x_1 \\ x_2 \\ \vdots \\ x_{N_t} \end{bmatrix} + \begin{bmatrix} n_1 \\ n_2 \\ \vdots \\ n_{N_r} \end{bmatrix} \tag{2.16}
$$

or, in matrix form, as

$$
\mathbf{r} = \mathbf{H}\mathbf{x} + \mathbf{n} \tag{2.17}
$$

where $\mathbf{r}$ represents an $N_r \times 1$ column matrix, $\mathbf{H}$ is an $N_r \times N_t$ matrix, $\mathbf{x}$ is an $N_t \times 1$ column matrix, and $\mathbf{n}$ is an $N_r \times 1$ column matrix [1].

Let each element in $\mathbf{x}$ be a zero-mean, independent identically distributed (IID) Gaussian random variable [1]. From information theory, the optimum distribution for transmitted signals is Gaussian, thus they are assumed to be Gaussian random variables [1]. The autocorrelation matrix $\mathbf{R}_{xx}$ of the transmitted signal $\mathbf{x}$ is defined by [1,4]

$$
\mathbf{R}_{xx} = E\left[\mathbf{x}\mathbf{x}^{*T}\right], \tag{2.18}
$$

where $\mathbf{A}^{*T}$ is the complex conjugate transpose of the matrix $\mathbf{A}$. Since $\mathbf{x}$ is a vector of zero-mean IID Gaussian random variables, they are uncorrelated [4,5]. The correlation matrix is diagonal. The covariance of $\mathbf{x}$ is given by [1,4]

$$
\mathbf{C}_{xx} = \mathbf{R}_{xx} . \tag{2.19}
$$

The total average power P of vector $\mathbf{x}$ is given by [1]

$$
P = \mathrm{E}\left[\sum_{j=1}^{N_t} \left|x_j\right|^2\right] = \sum_{j=1}^{N_t} \mathrm{E}\left[\left|x_j\right|^2\right] = \mathrm{tr}\left(\mathbf{R}_{xx}\right), \tag{2.20}
$$

where $\mathrm{tr}(\mathbf{A})$ is the trace of matrix $\mathbf{A}$, defined as the sum of its diagonal elements. It is assumed that each transmit antenna transmits equal power. The power from any one antenna is given by [1]

$$P_j = \mathrm{E}\left[\left|x_j\right|^2\right] = \frac{P}{N_t}. \tag{2.21}$$

Then $\mathbf{R}_{xx}$ is

$$\mathbf{R}_{xx} = \frac{P}{N_t}\mathbf{I}_{N_t}. \tag{2.22}$$

The symbol $\mathbf{I}_N$ represents the identity matrix of size N.

It was assumed in the previous section that the transmitted signal's bandwidth x_j is narrow enough that the frequency response of the channel is flat. Also we assume that there is no attenuation due to path loss or amplification due to antenna gain except as measured in the channel matrix $\mathbf{H}$. Furthermore, we assume that the channel representation matrix $\mathbf{H}$ is fixed during a symbol period, i.e., each element of $\mathbf{H}$ is a fixed coefficient. In the discussion of a multipath fading channel to follow, the appropriateness of these assumptions will be made clear.

Let the normalization constraints be [1]

$$\sum_{j=1}^{N_t}\left|h_{ij}\right|^2 = N_t \quad \text{for } i = 1, 2, \ldots N_r. \tag{2.23}$$

The sum of the magnitudes of each channel coefficient leading into any one receive antenna is N_t. If the channel coefficients are modeled as random variables, then the normalization constraint will apply to the expected value of the left hand side of Equation (2.23) [1]. This normalization is necessary for comparison to a SISO system.

The matrix $\mathbf{H}$ constitutes the channel state information (CSI). It is assumed that there is perfect knowledge of the CSI at the receiver. While this assumption is never true, it can be approached. For example, each coefficient can be estimated by sending training signals to the receiver [1].

The AWGN at each receive antenna is described by a single column matrix $\mathbf{n}$. The elements of $\mathbf{n}$ are zero-mean, equal variance, IID complex Gaussian random variables [1]. As with the transmitted signals, the autocorrelation matrix $\mathbf{n}$ is given by [1,4]

$$\mathbf{R}_{nn} = \mathrm{E}\left[\mathbf{n}\mathbf{n}^{*T}\right]. \tag{2.24}$$

Similar to the transmit matrix $\mathbf{x}$, since each element of the noise is assumed zero-mean, the covariance matrix is equal to the autocorrelation matrix. Each element of $\mathbf{n}$ is an IID random variable with equal variance; thus, they are independent and uncorrelated [5]. The power of each noise element is equal to the variance. The autocorrelation function is [1,4]

$$\mathbf{R}_{nn} = \sigma_o^2 \mathbf{I}_{N_r}. \tag{2.25}$$

Let the average power at each receive antenna in the absence of noise be represented by P_r which is given by [1,4]

$$\begin{aligned} P_r &= \mathrm{E}\left[r_i r_i^*\right] \\ &= \mathrm{E}\left[\sum_{j=1}^{N_t} h_{ij} x_j \sum_{k=1}^{N_t} h_{ik}^* x_k^*\right] \\ &= \mathrm{E}\left[\sum_{j=1}^{N_t}\sum_{k=1}^{N_t} h_{ij} x_j h_{ik}^* x_k^*\right] \\ &= \sum_{j=1}^{N_t}\sum_{k=1}^{N_t} h_{ij} h_{ik}^* \mathrm{E}\left[x_j x_k^*\right] \\ &= \sum_{j=1}^{N_t} \left|h_{ij}\right|^2 \mathrm{E}\left[\left|x_j\right|^2\right], \end{aligned} \tag{2.26}$$

where the channel coefficients have been assumed fixed, i.e., not random variables. The $(\ )^*$ represents the complex conjugate. Substitution of Equations (2.21) and (2.23) into Equation (2.26) gives

$$P_r = \sum_{j=1}^{N_t} \left|h_{ij}\right|^2 \mathrm{E}\left[\left|x_j\right|^2\right] = N_t \frac{P}{N_t} = P. \tag{2.27}$$

Then the average signal-to-noise ratio (SNR) at each receive antenna, represented by γ, is given by

$$\gamma = \frac{P}{\sigma_o^2}. \tag{2.28}$$

It was assumed that there was no path loss or gain through the channel with the exception of that measured by the channel coefficients. The total received power P_{tot} becomes

$$P_{tot} = \sum_{i}^{N_r} P = N_r P = \mathrm{tr}\left(R_{rr}\right). \tag{2.29}$$

The received signal autocorrelation matrix is

$$\mathbf{R}_{rr} = \mathrm{E}\left[\mathbf{r}\mathbf{r}^{*T}\right]. \tag{2.30}$$

Using Equation (2.17) in Equation (2.30), we obtain

$$\begin{aligned} \mathbf{R}_{rr} &= \mathrm{E}\left[\left(\mathbf{H}\mathbf{x}+\mathbf{n}\right)\left(\mathbf{H}\mathbf{x}+\mathbf{n}\right)^{*T}\right] \\ &= \mathrm{E}\left[\left(\mathbf{H}\mathbf{x}+\mathbf{n}\right)\left(\left(\mathbf{H}\mathbf{x}\right)^{*T}+\mathbf{n}^{*T}\right)\right]. \end{aligned} \tag{2.31}$$

Expansion of Equation (2.31) gives

$$\begin{aligned} \mathbf{R}_{rr} &= \mathrm{E}\left[\mathbf{H}\mathbf{x}\left(\mathbf{H}\mathbf{x}\right)^{*T}+\mathbf{H}\mathbf{x}\mathbf{n}^{*T}+\mathbf{n}\left(\mathbf{H}\mathbf{x}\right)^{*T}+\mathbf{n}\mathbf{n}^{*T}\right] \\ &= \mathrm{E}\left[\mathbf{H}\mathbf{x}\left(\mathbf{H}\mathbf{x}\right)^{*T}\right]+\mathrm{E}\left[\mathbf{H}\mathbf{x}\mathbf{n}^{*T}\right]+\mathrm{E}\left[\left(\mathbf{H}\mathbf{x}\right)^{*T}\mathbf{n}\right]+\mathrm{E}\left[\mathbf{n}\mathbf{n}^{*T}\right] \end{aligned} \tag{2.32}$$

since the expectation of a sum of random variables is the sum of expectations. The transposition of a product of matrices has the identity [6]

$$\left(\mathbf{H}\mathbf{x}\right)^{*T} = \mathbf{x}^{*T}\mathbf{H}^{*T}. \tag{2.33}$$

Then Equation (2.32) can be written as

$$\mathbf{R}_{rr} = \mathrm{E}\left[\mathbf{H}\mathbf{x}\mathbf{x}^{*T}\mathbf{H}^{*T}\right]+\mathrm{E}\left[\mathbf{H}\mathbf{x}\mathbf{n}^{*T}\right]+\mathrm{E}\left[\mathbf{x}^{*T}\mathbf{H}^{*T}\mathbf{n}\right]+\mathrm{E}\left[\mathbf{n}\mathbf{n}^{*T}\right]. \tag{2.34}$$

If $\mathbf{H}$ is deterministic and $\mathbf{x}$ and $\mathbf{n}$ are independent of each other, then they are also uncorrelated; thus,

$$\begin{aligned} \mathrm{E}\left[\mathbf{H}\mathbf{x}\mathbf{n}^{*T}\right] &= \mathbf{H}\mathrm{E}\left[\mathbf{x}\right]\mathrm{E}\left[\mathbf{n}^{*T}\right] \\ \mathrm{E}\left[\mathbf{x}^{*T}\mathbf{H}^{*T}\mathbf{n}\right] &= \mathrm{E}\left[\mathbf{x}^{*T}\right]\mathbf{H}^{*T}\mathrm{E}\left[\mathbf{n}\right]. \end{aligned} \tag{2.35}$$

Since both random variables $\mathbf{x}$ and $\mathbf{n}$ have zero-means, Equations (2.35) becomes

$$\begin{aligned} \mathrm{E}\left[\mathbf{H}\mathbf{x}\mathbf{n}^{*T}\right] &= 0 \\ \mathrm{E}\left[\mathbf{x}^{*T}\mathbf{H}^{*T}\mathbf{n}\right] &= 0, \end{aligned} \tag{2.36}$$

and Equation (2.34) reduces to

$$\mathbf{R}_{rr} = \mathbf{H}\mathrm{E}\left[\mathbf{x}\mathbf{x}^{*T}\right]\mathbf{H}^{*T} + \mathrm{E}\left[\mathbf{n}\mathbf{n}^{*T}\right]. \tag{2.37}$$

Substitution of Equations (2.18) and (2.24) into Equation (2.37) gives

$$\mathbf{R}_{rr} = \mathbf{H}\mathbf{R}_{xx}\,\mathbf{H}^{*T} + \mathbf{R}_{nn}\,. \tag{2.38}$$

Finally, there are two equations that define the MIMO model, Equations (2.17) and (2.38):

$$\begin{aligned} \mathbf{r} &= \mathbf{H}\mathbf{x} + \mathbf{n}, \\ \mathbf{R}_{rr} &= \mathbf{H}\mathbf{R}_{xx}\,\mathbf{H}^{*T} + \mathbf{R}_{nn}. \end{aligned} \tag{2.39}$$

The first is in terms of random vectors and the second is in terms of the autocorrelation matrices. With this information, the capacity of a MIMO system can be derived.

C. CAPACITY OF MIMO SYSTEMS

The derivation of the capacity of MIMO systems presented here is roughly drawn from that found in Reference [1]. First, consider Equation (2.17)

$$\mathbf{r} = \mathbf{H}\mathbf{x} + \mathbf{n}\,. \tag{2.40}$$

Any $N_r \times N_t$ matrix $\mathbf{H}$ can be decomposed by the singular value decomposition (SVD) theorem into a product of matrices [4]

$$\mathbf{H} = \mathbf{U}\mathbf{D}\mathbf{V}^{*T}\,. \tag{2.41}$$

For reference, the matrix $\mathbf{Q}$ is defined by [1]

$$\mathbf{Q} = \begin{cases} \mathbf{H}\mathbf{H}^{*T} & \text{when } N_r < N_t \\ \mathbf{H}^{*T}\mathbf{H} & \text{when } N_t \le N_r. \end{cases} \tag{2.42}$$

Note that the singular values of $\mathbf{H}$ are defined to be the square roots of the eigenvalues of $\mathbf{Q}$ [1,4]. Let the eigenvalues of $\mathbf{Q}$ be represented by λ_i where $i = 1, 2, 3\ldots$. Now, Equation (2.40) can be rewritten as

$$\mathbf{r} = \mathbf{U}\mathbf{D}\mathbf{V}^{*T}\mathbf{x} + \mathbf{n}. \tag{2.43}$$

The matrices $\mathbf{D}$, $\mathbf{U}$ and $\mathbf{V}$ have the following properties [1,4]. Matrix $\mathbf{D}$ is an $N_r \times N_t$ matrix of nonnegative, real, singular values of $\mathbf{H}$. Let the singular values of $\mathbf{H}$ be represented by ρ_i. Then the matrix $\mathbf{D}$ is given by

$$\mathbf{D} = \begin{bmatrix} \rho_1 & 0 & \cdots & 0 \\ 0 & \rho_2 & \cdots & 0 \\ \vdots & \vdots & \ddots & \vdots \\ 0 & 0 & \cdots & \rho_{N_t} \\ 0 & 0 & \cdots & 0 \\ \vdots & \vdots & \ddots & \vdots \\ 0 & 0 & \cdots & 0 \end{bmatrix} \quad \text{when } N_t < N_r, \tag{2.44}$$

$$\mathbf{D} = \begin{bmatrix} \rho_1 & 0 & \cdots & 0 & \cdots & 0 \\ 0 & \rho_2 & \cdots & 0 & \cdots & 0 \\ \vdots & \vdots & \ddots & \vdots & \ddots & \vdots \\ 0 & 0 & \cdots & \rho_{N_r} & \cdots & 0 \end{bmatrix} \quad \text{when } N_r < N_t, \tag{2.45}$$

$$\mathbf{D} = \begin{bmatrix} \rho_1 & 0 & \cdots & 0 \\ 0 & \rho_2 & \cdots & 0 \\ \vdots & \vdots & \ddots & \vdots \\ 0 & 0 & \cdots & \rho_N \end{bmatrix} \quad \text{when } N_t = N_r = N. \tag{2.46}$$

Making the assumption that

$$\rho_1 \geq \rho_2 \ldots \geq \rho_N , \tag{2.47}$$

it is seen that some of the higher numbered ρ_n can be zero. If the rank of $\mathbf{H}$ is r, then there are r nonzero singularities [4]. The matrix $\mathbf{U}$ is an $N_r \times N_r$ unitary matrix comprised of the left singular vectors of $\mathbf{H}$ [1,4]

$$\mathbf{U} = \begin{bmatrix} & & \cdots & \\ \mathbf{u}_1 & \mathbf{u}_2 & \ddots & \mathbf{u}_{N_r} \\ & & \cdots & \end{bmatrix}. \tag{2.48}$$

The left singular vectors of $\mathbf{U}$, represented as $\mathbf{u_1}, \mathbf{u_2} \ldots \mathbf{u}_{N_r}$, are defined as the eigenvectors of $\mathbf{H}\mathbf{H}^{*T}$ [1,4]. The matrix $\mathbf{V}$ is an $N_t \times N_t$ unitary matrix comprised of right singular vectors of $\mathbf{H}$ given by

$$\mathbf{V} = \begin{bmatrix} & & \cdots & \\ \mathbf{v}_1 & \mathbf{v}_2 & \ddots & \mathbf{v}_{N_t} \\ & & \cdots & \end{bmatrix}. \tag{2.49}$$

The right singular vectors of $\mathbf{V}$, represented as $\mathbf{v_1}, \mathbf{v_2} \ldots \mathbf{v}_{N_t}$ are defined as the eigenvectors of $\mathbf{H}^{*T}\mathbf{H}$ [1,4]. Lastly, a unitary matrix $\mathbf{A}$ has the following properties [6]:

$$\begin{aligned} \mathbf{A}^T &= \left(\mathbf{A}^*\right)^{-1} \\ \mathbf{A}^{*T} &= \mathbf{A}^{-1}, \end{aligned} \tag{2.50}$$

and

$$\mathbf{A}\mathbf{A}^{*T} = \mathbf{A}\mathbf{A}^{-1} = \mathbf{I} . \tag{2.51}$$

Both matrices $\mathbf{U}$ and $\mathbf{V}$ have these properties.

Let the following transformations take place on $\mathbf{r}$, $\mathbf{x}$ and $\mathbf{n}$ [1]:

$$\begin{aligned} \mathbf{r}' &= \mathbf{U}^{*T}\mathbf{r}, \\ \mathbf{x}' &= \mathbf{V}^{*T}\mathbf{x}, \\ \mathbf{n}' &= \mathbf{U}^{*T}\mathbf{n}. \end{aligned} \tag{2.52}$$

Then

$$\begin{aligned}\mathbf{r} &= \left(\mathbf{U}^{*T}\right)^{-1}\mathbf{r}',\\ \mathbf{x} &= \left(\mathbf{V}^{*T}\right)^{-1}\mathbf{x}',\\ \mathbf{n} &= \left(\mathbf{U}^{*T}\right)^{-1}\mathbf{n}'.\end{aligned} \tag{2.53}$$

Substitution of Equations (2.53) into Equation (2.43) gives

$$\left(\mathbf{U}^{*T}\right)^{-1}\mathbf{r}' = \mathbf{U}\mathbf{D}\mathbf{V}^{*T}\left(\mathbf{V}^{*T}\right)^{-1}\mathbf{x}' + \left(\mathbf{U}^{*T}\right)^{-1}\mathbf{n}'. \tag{2.54}$$

Multiplying both sides of this equation by $\mathbf{U}^{*T}$ and using the properties defined in Equation (2.50) and (2.51), we obtain

$$\begin{aligned}&\mathbf{U}^{*T}\left(\mathbf{U}^{*T}\right)^{-1}\mathbf{r}' = \mathbf{U}^{*T}\mathbf{U}\mathbf{D}\mathbf{V}^{*T}\left(\mathbf{V}^{*T}\right)^{-1}\mathbf{x}' + \mathbf{U}^{*T}\left(\mathbf{U}^{*T}\right)^{-1}\mathbf{n}'\\ &\mathbf{I}\mathbf{r}' = \mathbf{I}\mathbf{D}\mathbf{I}\mathbf{x}' + \mathbf{I}\mathbf{n}'\\ &\mathbf{r}' = \mathbf{D}\mathbf{x}' + \mathbf{n}'.\end{aligned} \tag{2.55}$$

Therefore, Equation (2.55) is an equivalent representation of Equation (2.40).

Expanding Equation (2.55) when $N_t \le N_r$, we get

$$\begin{bmatrix} r_1' \\ r_2' \\ \vdots \\ r_{N_t}' \\ r_{N_t+1}' \\ \vdots \\ r_{N_r}' \end{bmatrix} = \begin{bmatrix} \sqrt{\lambda_1} & 0 & \cdots & 0 \\ 0 & \sqrt{\lambda_2} & \cdots & 0 \\ \vdots & \vdots & \ddots & \vdots \\ 0 & 0 & \cdots & \sqrt{\lambda_{N_t}} \\ 0 & 0 & \cdots & 0 \\ \vdots & \vdots & \ddots & \vdots \\ 0 & 0 & \cdots & 0 \end{bmatrix} \begin{bmatrix} x_1' \\ x_2' \\ \vdots \\ x_{N_t}' \end{bmatrix} + \begin{bmatrix} n_1' \\ n_2' \\ \vdots \\ n_{N_t}' \\ n_{N_t+1}' \\ \vdots \\ n_{N_r}' \end{bmatrix}. \tag{2.56}$$

Similarly, when $N_r < N_t$, Equation (2.55) expands to

$$\begin{bmatrix} r_1' \\ r_2' \\ \vdots \\ r_{N_r}' \end{bmatrix} = \begin{bmatrix} \sqrt{\lambda_1} & 0 & \cdots & 0 & \cdots & 0 \\ 0 & \sqrt{\lambda_2} & \cdots & 0 & \cdots & 0 \\ \vdots & \vdots & \ddots & \vdots & \ddots & \vdots \\ 0 & 0 & \cdots & \sqrt{\lambda_{N_r}} & \cdots & 0 \end{bmatrix} \begin{bmatrix} x_1' \\ x_2' \\ \vdots \\ x_{N_r}' \\ x_{N_r+1}' \\ \vdots \\ x_{N_t}' \end{bmatrix} + \begin{bmatrix} n_1' \\ n_2' \\ \vdots \\ n_{N_r}' \end{bmatrix}. \qquad (2.57)$$

Equations (2.56) and (2.57) are described graphically in Figure 4 and Figure 5.

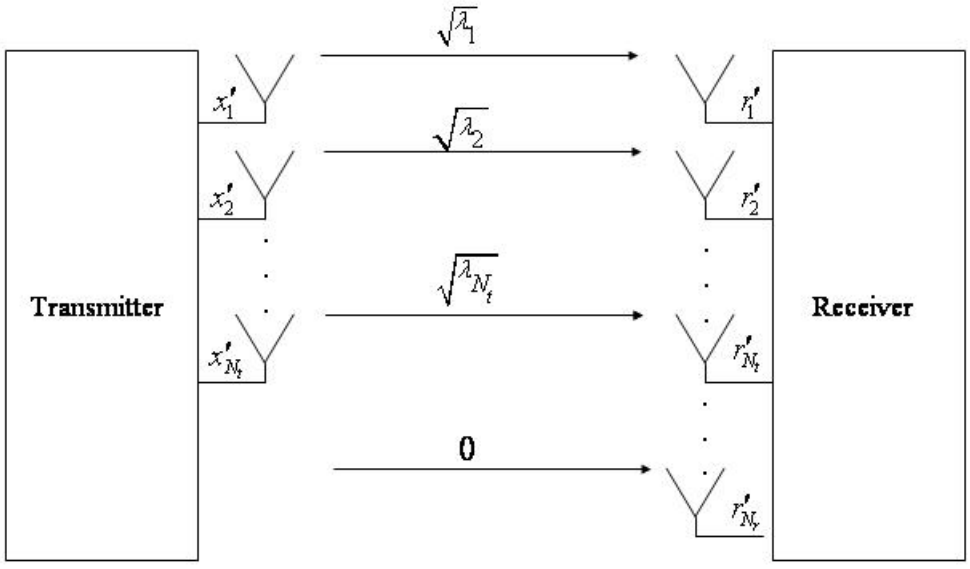

Figure 4. The equivalent MIMO model $N_t \le N_r$ (After Reference [1].).

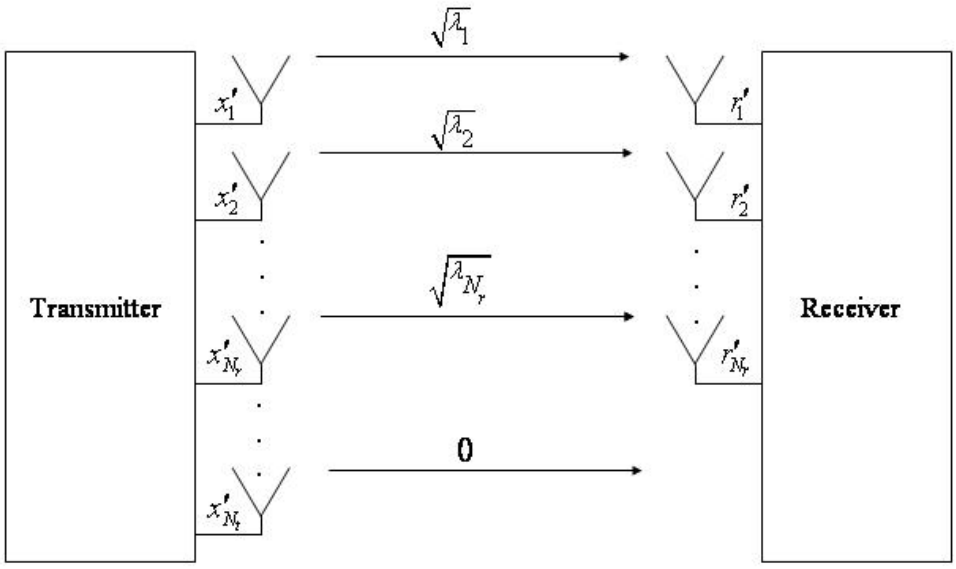

Figure 5. The equivalent MIMO model $N_r < N_t$ (After Reference [1].).

Note that the 0 in Figures 4 and 5 means that no signal passes in that channel. For either situation, $N_t \le N_r$ or $N_r < N_t$, the equivalent received signal at any receive antenna, where r is the rank of $\mathbf{H}$, is

$$r_i' = \sqrt{\lambda_i}\, x_i' + n_i' \qquad \text{where } i = 1, 2, \ldots r. \tag{2.58}$$

The rank of $\mathbf{H}$ can be no larger than the minimum value between N_t and N_r [1,4,6]. Furthermore, from Figures 4 and 5 and Equation (2.58), it can be seen that the equivalent received signal at any receive antenna r_i' is a direct couple between the equivalent transmit signal x_i' with an applied gain factor $\sqrt{\lambda_i}$, a singular value of $\mathbf{H}$. No longer are the received signals a linear sum of all transmit signals multiplied by a channel coefficient, as was the case in the general MIMO model.

The equivalent channel describes r direct uncoupled SISO channels. The capacity of the system as a whole is just the sum of the individual capacities [1]. Shannon's capacity equation is [7]

$$C = W \log_2 \left[1 + \mathrm{SNR}\right], \tag{2.59}$$

where C is the capacity in information bits/second, W is the bandwidth of the channel in Hertz and SNR is the signal-to-noise ratio. Thus, the capacity of the MIMO system is given by

$$C = W\sum_{i=1}^{r}\log_2\left[1+\mathrm{SNR}_i'\right], \tag{2.60}$$

where SNR_i' is the signal-to-noise ratio for the *i*-th equivalent channel. To determine the maximum spectral efficiency C/W, it is sufficient to find the equivalent received signal and noise power. The equivalent received power in the *i*-th channel is the power of the transmitted signal multiplied by the associated eigenvalue. In order to obtain the power of $\mathbf{x}'$, the autocorrelation matrix is found; that is,

$$\mathbf{R}_{x'x'} = \mathrm{E}\left[\mathbf{x}'\mathbf{x}'^{*T}\right]. \tag{2.61}$$

The substitution of Equation (2.52) into Equation (2.61) gives

$$\mathbf{R}_{x'x'} = \mathrm{E}\left[\mathbf{V}^{*T}\mathbf{x}\left(\mathbf{V}^{*T}\mathbf{x}\right)^{*T}\right]. \tag{2.62}$$

Using the transposition identity defined in Equation (2.33), we see that Equation (2.62) reduces to

$$\begin{aligned}\mathbf{R}_{x'x'} &= \mathrm{E}\left[\mathbf{V}^{*T}\mathbf{x}\mathbf{x}^{*T}\mathbf{V}\right]\\ &= \mathbf{V}^{*T}\mathrm{E}\left[\mathbf{x}\mathbf{x}^{*T}\right]\mathbf{V}\\ &= \mathbf{V}^{*T}\mathbf{R}_{xx}\mathbf{V}.\end{aligned} \tag{2.63}$$

Substitution of Equation (2.22) in Equation (2.63) gives

$$\begin{aligned}\mathbf{R}_{x'x'} &= \mathbf{V}^{*T}\frac{P}{Nt}\mathbf{I}_{N_t}\mathbf{V}\\ &= \frac{P}{N_t}\mathbf{V}^{*T}\mathbf{I}_{N_t}\mathbf{V}.\end{aligned} \tag{2.64}$$

The matrix $\mathbf{V}$ is an $N_t \times N_t$ unitary matrix; using the identity in Equation (2.51), we see that Equation (2.64) reduces to

$$\mathbf{R}_{x'x'} = \frac{P}{N_t}\mathbf{I}_{N_t}. \tag{2.65}$$

Similarly, to find the power of the equivalent noise the autocorrelation of $\mathbf{n}'$ is used, which is defined as

$$\mathbf{R}_{n'n'} = \mathrm{E}\left[\mathbf{n}'\mathbf{n}'^{*T}\right]. \tag{2.66}$$

Once again, substituting the transformation defined in Equation (2.52), we get

$$\begin{aligned}\mathbf{R}_{n'n'} &= \mathrm{E}\left[\mathbf{U}^{*T}\mathbf{n}\left(\mathbf{U}^{*T}\mathbf{n}\right)^{*T}\right] \\ &= \mathrm{E}\left[\mathbf{U}^{*T}\mathbf{n}\mathbf{n}^{*T}\mathbf{U}\right] \\ &= \mathbf{U}^{*T}\mathbf{R}_{nn}\mathbf{U}.\end{aligned} \tag{2.67}$$

The substitution of Equation (2.25) into Equation (2.67) gives

$$\mathbf{R}_{n'n'} = \mathbf{U}^{*T}\sigma_o^2\mathbf{I}_{N_r}\mathbf{U}. \tag{2.68}$$

The matrix $\mathbf{U}$ is an $N_r \times N_r$ unitary matrix; using the identity in Equation (2.51), we see that Equation (2.68) reduces to

$$\mathbf{R}_{n'n'} = \sigma_o^2\mathbf{I}_{N_r}. \tag{2.69}$$

Therefore, the SNR of the *i*-th equivalent channel is

$$\mathrm{SNR}_i' = \frac{\lambda_i P}{N_t\sigma_o^2}. \tag{2.70}$$

Using Equation (2.70) and (2.60), we find the capacity of the MIMO system to be

$$\begin{aligned}C &= W\sum_{i=1}^{r}\log_2\left[1+\frac{\lambda_i P}{N_t\sigma_o^2}\right] \\ &= W\log_2\prod_{i=1}^{r}\left[1+\frac{\lambda_i P}{N_t\sigma_o^2}\right],\end{aligned} \tag{2.71}$$

where λ_i are the eigenvalues of $\mathbf{Q}$ and r is the rank of $\mathbf{H}$, assumed to be given by

$$r = \min(N_r, N_t). \tag{2.72}$$

The function $\min(N_r, N_t)$ represents the minimum between N_r and N_t.

Ideally, Equation (2.71) should be in terms of the channel matrix $\mathbf{H}$. Let the eigenvalue equation be defined by [1,6]

$$\left(\lambda \mathbf{I}_r - \mathbf{Q}\right)\mathbf{y} = \mathbf{0} \qquad \text{where } \mathbf{y} \neq 0. \tag{2.73}$$

The matrix $\mathbf{Q}$ is defined in Equation (2.42).

$$\mathbf{Q} = \begin{cases} \mathbf{H}\mathbf{H}^{*T} & \text{when } N_r < N_t \\ \mathbf{H}^{*T}\mathbf{H} & \text{when } N_t \leq N_r. \end{cases} \tag{2.74}$$

Equation (2.73) has a non-trivial solution if λ is the root of the characteristic equation [6]. The characteristic equation is

$$p(\lambda) = \det\left(\lambda \mathbf{I}_r - \mathbf{Q}\right) = 0. \tag{2.75}$$

The eigenvalues of a square matrix $\mathbf{Q}$ are the roots of the characteristic equation $p(\lambda)$; therefore, the solution to $p(\lambda)$ can be written as [6]

$$\begin{aligned} p(\lambda) &= (\lambda - \lambda_1)(\lambda - \lambda_2)\cdots(\lambda - \lambda_r) = 0 \\ &= \prod_{i=1}^{r} (\lambda - \lambda_i) = 0, \end{aligned} \tag{2.76}$$

where $\lambda_1, \lambda_2, \ldots, \lambda_r$ are the eigenvalues of $\mathbf{Q}$. Combining Equation (2.75) and (2.76), we get

$$\prod_{i=1}^{r} (\lambda - \lambda_i) = \det\left(\lambda \mathbf{I}_r - \mathbf{Q}\right). \tag{2.77}$$

This is true for all values of λ in the real domain [1,4].

Noting the similarities of the left hand side of Equation (2.77) to (2.71) and making the substitution defined by [1]

$$\lambda = -\frac{N_t \sigma_o^2}{P} \tag{2.78}$$

in Equation (2.77), we get

$$\prod_{i=1}^{r}(-\frac{N_t\sigma_o^2}{P}-\lambda_i)=\det\left(-\frac{N_t\sigma_o^2}{P}\mathbf{I}_r-\mathbf{Q}\right)$$
$$\prod_{i=1}^{r}(1+\frac{\lambda_i P}{N_t\sigma_o^2})=\det\left(\mathbf{I}_r+\frac{P}{N_t\sigma_o^2}\mathbf{Q}\right). \tag{2.79}$$

Therefore, the equation for the capacity of a MIMO system becomes

$$C=W\log_2\prod_{i=1}^{r}\left[1+\frac{\lambda_i P}{N_t\sigma_o^2}\right]$$
$$C=W\log_2\left(\det\left(\mathbf{I}_r+\frac{P}{N_t\sigma_o^2}\mathbf{Q}\right)\right). \tag{2.80}$$

It is appropriate to discuss three examples to illustrate the result. For the first example, let the system be a SISO system, i.e., a system with a single transmit and a single receive antenna. From Equation (2.59), the normalized capacity, i.e., the maximum spectral efficiency, becomes

$$\frac{C}{W}=\log_2\left[1+\mathrm{SNR}\right]. \tag{2.81}$$

Let the SNR be 10.0 dB. Thus the normalized capacity is 3.46 bit/s/Hz.

For the same example but this time Equation (2.80) is used. In this case $\mathbf{Q}=1, \mathbf{I}_r=1$ and $N_t=1$. Using this information in Equation (2.80), we get

$$C=W\log_2\left(\det\left(1+\frac{P}{\sigma_o^2}\right)\right)$$
$$\frac{C}{W}=\log_2\left(1+\frac{P}{\sigma_o^2}\right) \tag{2.82}$$
$$\frac{C}{W}=\log_2\left(1+\mathrm{SNR}\right).$$

Thus, Equation (2.80) reduces to Equation (2.81).

For the next example, consider a MIMO system with the same number of transmit and receive antennas, that is, $N_t=N_r=N$. Let the channel matrix $\mathbf{H}$ be defined by [1]

$$\mathbf{H} = \begin{bmatrix} \sqrt{N} & 0 & 0 & \cdots & 0 \\ 0 & \sqrt{N} & 0 & \cdots & 0 \\ \vdots & \cdots & \ddots & & \vdots \\ 0 & 0 & 0 & \cdots & \sqrt{N} \end{bmatrix}. \tag{2.83}$$

This is equivalent to N independent, uncoupled SISO channels. The matrix $\mathbf{Q}$ is defined by $\mathbf{H}^{*T}\mathbf{H}$ and given by,

$$\begin{aligned} \mathbf{Q} &= \begin{bmatrix} N & 0 & 0 & \cdots & 0 \\ 0 & N & 0 & \cdots & 0 \\ \vdots & \cdots & \ddots & & \vdots \\ 0 & 0 & 0 & \cdots & N \end{bmatrix} \\ &= N\mathbf{I}_N. \end{aligned} \tag{2.84}$$

Using Equation (2.80), we find the normalized capacity to be

$$\frac{C}{W} = \log_2\left(\det\left(\mathbf{I}_n + \frac{P}{N\sigma_o^2}\mathbf{Q}\right)\right). \tag{2.85}$$

Substituting Equation (2.84) into Equation (2.85), we get

$$\begin{aligned} \frac{C}{W} &= \log_2\left(\det\left(\mathbf{I}_N + \frac{NP}{N\sigma_o^2}\mathbf{I}_N\right)\right) \\ &= \log_2\left(\det\left(\mathbf{I}_N + \frac{P}{\sigma_o^2}\mathbf{I}_N\right)\right) \\ &= \log_2\left(\det\left(\left(1 + \frac{P}{\sigma_o^2}\right)\mathbf{I}_N\right)\right). \end{aligned} \tag{2.86}$$

Since the determinant of a diagonal matrix is the product of the diagonals [8], Equation (2.86) becomes

$$\begin{aligned} \frac{C}{W} &= \log_2\left(1 + \frac{P}{\sigma_o^2}\right)^N \\ &= N\log_2\left(1 + \frac{P}{\sigma_o^2}\right). \end{aligned} \tag{2.87}$$

The capacity of the channel using a MIMO system as defined by matrix $\mathbf{H}$ in Equation (2.83) gives a capacity N times that of the SISO case. This makes sense since the channel is equivalent to N independent SISO channels. The capacity increases linearly with the number of antennas. If $N = 2$, then the normalized capacity for SNR of 10.0 dB is 6.92 bits/s/Hz.

Lastly, consider the 2×2 matrix $\mathbf{H}$ given by

$$\mathbf{H} = \begin{bmatrix} e^{j\phi} & -e^{-j\theta} \\ e^{j\theta} & e^{-j\phi} \end{bmatrix}. \tag{2.88}$$

This represents a MIMO system with $N_t = N_r = 2$. The channel coefficients are fixed. The matrix $\mathbf{Q}$ is defined by $\mathbf{H}^{*T}\mathbf{H}$ and given by

$$\begin{aligned} \mathbf{H}^{*T}\mathbf{H} &= \begin{bmatrix} e^{-j\phi} & e^{-j\theta} \\ -e^{j\theta} & e^{j\phi} \end{bmatrix} \begin{bmatrix} e^{j\phi} & -e^{-j\theta} \\ e^{j\theta} & e^{-j\phi} \end{bmatrix} \\ &= \begin{bmatrix} 2 & 0 \\ 0 & 2 \end{bmatrix}. \end{aligned} \tag{2.89}$$

Then Equation (2.80) becomes

$$\begin{aligned} C &= W \log_2 \left(\det \left(\mathbf{I}_2 + \frac{P}{\sigma_o^2} \mathbf{I}_2 \right) \right) \\ \frac{C}{W} &= 2 \log_2 \left(1 + \frac{P}{\sigma_o^2} \right). \end{aligned} \tag{2.90}$$

The capacity of the channel using this matrix $\mathbf{H}$ gives the same result as the previous example when $N = 2$. The capacity in this case also increases linearly with the number of antennas. If $N = 2$ then the normalized capacity for the same SNR, 10.0 dB, is 6.92 bits/s/Hz. If the $\mathbf{Q}$ matrix can be reduced to a scalar multiplied by the identity matrix, then capacity is linearly proportional to the number of transmit antennas, maximizing the possible capacity of the system.

D. THE MULTITPATH FADING CHANNEL

The worst channel for any type of wireless digital communication system is the multipath fading channel. Performance in this type of channel is much less than that of AWGN alone [9,10,11]. In this section, an overview of the multipath fading channel is presented. The MIMO system design will be tested in this channel. Consequently, a model of this channel is derived in baseband equivalent form for use in the simulation.

Firstly, radio waves may travel from a transmit antenna to a receive antenna by several different paths. This is called multipath. Multipath propagation of the signal is caused by reflectors and scatters present in the physical channel [9,10,11]. The signal, traveling via several different paths, will be sensed at the receive antenna several different times with different amplitudes, phases and arrival times [9,11]. This results in a received signal that can vary dramatically in amplitude and phase. In the frequency domain, the spectral components of the signal may be affected differently by the channel. Thus, the frequency response of the channel may not be flat over the bandwidth of the signal. The overall result of multipath propagation is time–spreading of the signal that leads to intersymbol interference [9,10].

The configuration of the reflectors and scatters in the physical channel may change over time as well. This can be caused by the reflectors and scatters moving, or more likely, the transmit or receive antennas moving. As a result, the multipath channel is time–varying. The motion between the transmitter and receive antennas will cause a Doppler shift in frequency proportional to the relative velocity between them [9,10,11].

The time–spreading and time–varying aspects of the multipath fading channel can be measured and statistically estimated [9,10,11]. A maximum for the Doppler shift can be determined as well. Knowledge of this information aids the engineer in making key design decisions for a communication system.

The time–spreading nature of the channel is characterize by the coherence bandwidth. "The coherence bandwidth is a statistical measure over which the frequency response of the channel is considered flat" [11]. The spectral components of a signal that fit in the coherence bandwidth will be passed with generally equal gain and linear phase. If a signal spectrum fits within the coherence bandwidth, then it undergoes flat fading.

Thus, the channel is flat fading or frequency–nonselective. If the spectrum does not fit within the coherence bandwidth, then it suffers frequency selective fading. Thus, the channel is frequency–selective [11].

The time–varying nature of the channel is described by the Doppler spread and coherence time [9,10,11]. The coherence time is inversely proportional to the maximum doppler shift [9,10,11]. The coherence time is the statistical measure of the duration during which the channel is essentially time–invariant. Thus, the coherence time gives an indication of how long the channel remains constant. If the symbol duration of a signal is less than the coherence time, then it undergoes slow fading. Thus, the channel is called slowly fading. If the symbol duration is larger than the coherence time, then the signal suffers fast fading and the channel is called fast fading [9,10,11].

The simulations were run for a slow fading, frequency–nonselective channel. To simulate a slow fading channel, the model of the channel coefficients is not permitted to change within a symbol period. This corresponds to the assumptions made concerning the channel coefficients in Sections A and B. In order to simulate the frequency–nonselective or flat fading nature of the channel, the channel coefficients must be distributed according to a probability distribution function. Flat fading is generally simulated using a Rayleigh distribution for the magnitude of the channel coefficients [9,10,11]. This is consistent with a channel where the fading is caused by randomly moving scatterers and reflectors or moving transmitter and receiver. In order to achieve the baseband simulation of a Rayleigh distribution, two zero-mean, independent Gaussian random variables are summed [11].

Let Z be the complex sum of two IID, zero-mean Gaussian random variables given by

$$Z = X + jY = He^{j\theta}. \tag{2.91}$$

The mean and variance of X and Y are

$$\overline{X} = \overline{Y} = 0, \tag{2.92}$$

$$\sigma_x^2 = \sigma_y^2 = \sigma^2. \tag{2.93}$$

Let W be

$$W = |Z|^2 , \tag{2.94}$$

or, equivalently

$$W = X^2 + Y^2 . \tag{2.95}$$

The random variable W has a chi-squared distribution given by [10]

$$f_W(w) = \frac{1}{\sigma^n 2^{n/2} \Gamma\left(\frac{n}{2}\right)} w^{(n/2)-1} e^{-w/2\sigma^2} u(w), \tag{2.96}$$

where the unit step function is denoted by

$$u(w) = \begin{cases} 0 & w < 0 \\ 1 & w \geq 0. \end{cases} \tag{2.97}$$

The variable n is defined as the number of independent random variables in the sum. In this case $n = 2$. The distribution then becomes

$$f_W(w) = \frac{1}{\sigma^2 2^{2/2} \Gamma\left(\frac{2}{2}\right)} w^{(2/2)-1} e^{-w/2\sigma^2} u(w) . \tag{2.98}$$

This reduces to

$$f_W(w) = \frac{1}{\sigma^2 2\Gamma(1)} w^0 e^{-w/2\sigma^2} u(w) . \tag{2.99}$$

Since

$$\Gamma(1) = (1-1)! = 1 , \tag{2.100}$$

the probability distribution function of W is given by

$$f_W(w) = \frac{1}{2\sigma^2} e^{-w/2\sigma^2} u(w) . \tag{2.101}$$

The magnitude H of Z in Equation (2.91) is of interest and is given by

$$H = |Z| = \sqrt{W} \,. \tag{2.102}$$

The probability density function for W can be transformed to yield the probability density function of H according to [12]

$$f_H(h) = \frac{1}{|dh/dw|} f_W(w)\Big|_{w=h^2}, \tag{2.103}$$

where

$$\frac{dh}{dw} = \frac{1}{2(w)^{1/2}} \,. \tag{2.104}$$

Using Equation (2.101) and the substitution defined in Equation (2.104) in Equation (2.103), we get

$$\begin{aligned} f_H(h) &= 2(h^2)^{1/2} \frac{1}{2\sigma^2} e^{-h^r/2\sigma^2} u(h) \\ f_H(h) &= \frac{h}{\sigma^2} e^{-h^2/2\sigma^2} u(h). \end{aligned} \tag{2.105}$$

The mean and variance of H are given by [11]

$$\begin{aligned} \overline{h} &= \sigma\sqrt{\frac{\pi}{2}} \\ \sigma_h^2 &= \sigma^2\left(2 - \frac{\pi}{2}\right). \end{aligned} \tag{2.106}$$

Thus, H follows a Rayleigh distribution as required, and the sum of two zero-mean, IID Gaussian noise sources will produce the desired channel model.

The phase Θ of Z is given by

$$\Theta = \begin{cases} \tan^{-1}\left(\frac{Y}{X}\right) - \pi & \text{for } -\infty \le x < 0, -\infty \le y \le 0 \\ \tan^{-1}\left(\frac{Y}{X}\right) & \text{for } 0 < x \le \infty, -\infty \le y \le \infty \\ \tan^{-1}\left(\frac{Y}{X}\right) + \pi & \text{for } -\infty \le x < 0, 0 \le y \le \infty. \end{cases} \tag{2.107}$$

Let A be

$$A = \frac{Y}{X}. \tag{2.108}$$

For the first case, when $-\infty \le x < 0, -\infty \le y \le 0$, the cumulative distribution function is given by [5]

$$F_A(a) = \int_{-\infty}^{0}\int_{ax}^{0} f_{XY}(x,y)\,dy\,dx. \tag{2.109}$$

The probability distribution function is given by taking the derivative of $F_A(a)$

$$\frac{dF_A(a)}{da} = \frac{d}{da}\left[\int_{-\infty}^{0}\int_{ax}^{0} f_{XY}(x,y)\,dy\,dx\right]. \tag{2.110}$$

By the Leibniz rule, the probability density function is given by [5]

$$f_A(a) = \int_{-\infty}^{0} -x f_{XY}(x, ax)\,dx. \tag{2.111}$$

The random variables X and Y are independent; therefore their joint probability density function is given by

$$f_{XY}(x,y) = f_X(x) f_Y(y). \tag{2.112}$$

The substitutions of Equation (2.112) as well as the Gaussian probability density function into (2.111) gives

$$f_A(a) = -\frac{1}{4\pi\sigma^2}\left[\int_{-\infty}^{0} e^{-x^2\left(\frac{1+a^2}{2\sigma^2}\right)}(2x)\,dx\right]. \tag{2.113}$$

Evaluating Equation (2.113), we obtain

$$f_A(a) = \frac{1}{2\pi\left(1+a^2\right)} \quad 0 \le a \le \infty . \tag{2.114}$$

The random variable Θ is given by

$$\Theta = \tan^{-1}(A) - \pi , \tag{2.115}$$

where

$$\left|\frac{d\theta}{da}\right| = \frac{1}{1+a^2} , \tag{2.116}$$

and

$$a = \tan(\theta + \pi) . \tag{2.117}$$

Using the transform defined in (2.103), we get

$$f_\Theta(\theta) = 1 + a^2 \left.\frac{1}{2\pi\left(1+a^2\right)}\right|_{a=\tan(\theta)} . \tag{2.118}$$

Equation (2.118) simplifies to

$$f_\Theta(\theta) = \frac{1}{2\pi} \quad \text{for } -\pi \le \theta \le -\frac{\pi}{2} . \tag{2.119}$$

For the second case, when $0 < x \le \infty, -\infty \le y \le \infty$, the cumulative distribution function is given by [5]

$$F_A(a) = \int_0^\infty \int_{-\infty}^{ax} f_{XY}(x,y)\, dy dx . \tag{2.120}$$

Like the first case, the probability distribution function is gained by taking the derivative of $F_A(a)$

$$\frac{dF_A(a)}{da} = \frac{d}{da}\left[\int_0^\infty \int_{-\infty}^{ax} f_{XY}(x,y)\, dy dx\right] . \tag{2.121}$$

By the Leibniz rule, the probability density function is [5]

$$f_A(a) = \int_0^\infty x f_{XY}(x, ax)\, dx. \tag{2.122}$$

Similar to the first case first case, $f_A(a)$ is

$$f_A(a) = \frac{1}{2\pi\left(1+a^2\right)} \quad -\infty \le a \le \infty. \tag{2.123}$$

In this case Θ is given by

$$\Theta = \tan^{-1}(A), \tag{2.124}$$

where

$$\left|\frac{d\theta}{da}\right| = \frac{1}{1+a^2}, \tag{2.125}$$

and

$$a = \tan(\theta). \tag{2.126}$$

After transformation $f_\Theta(\theta)$ becomes

$$f_\Theta(\theta) = \frac{1}{2\pi} \quad \text{for } -\frac{\pi}{2} \le \theta \le \frac{\pi}{2}. \tag{2.127}$$

For the last case, when $-\infty \le x < 0, -\infty \le y \le 0$, the cumulative distribution function is given by [5]

$$F_A(a) = \int_{-\infty}^0 \int_{ax}^\infty f_{XY}(x, y)\, dy dx. \tag{2.128}$$

The probability distribution function is given by taking the derivative of $F_A(a)$

$$\frac{dF_A(a)}{da} = \frac{d}{da}\left[\int_{-\infty}^0 \int_{ax}^\infty f_{XY}(x, y)\, dy dx\right]. \tag{2.129}$$

Once again, by Leibniz's rule, the probability density function is [5]

$$f_A(a) = \int_0^\infty -x f_{XY}(x, ax)\, dx, \tag{2.130}$$

and $f_A(a)$ becomes

$$f_A(a) = \frac{1}{2\pi\left(1+a^2\right)} \quad -\infty \le a \le 0\,. \tag{2.131}$$

In this case Θ is given by

$$\Theta = \tan^{-1}(A) + \pi\,, \tag{2.132}$$

where

$$\left|\frac{d\theta}{da}\right| = \frac{1}{1+a^2}\,, \tag{2.133}$$

and

$$a = \tan(\theta)\,. \tag{2.134}$$

Finally, after transformation $f_\Theta(\theta)$ becomes

$$f_\Theta(\theta) = \frac{1}{2\pi} \quad \text{for } \frac{\pi}{2} \le \theta \le \pi\,. \tag{2.135}$$

Therefore, the complex sum of two zero-mean, IID Gaussian random variables gives a magnitude that is Rayleigh distributed with a phase that is uniformly distributed in $[-\pi, \pi]$. This models the baseband equivalent slow fading, frequency–nonselective channel. It will be used to simulate a multipath fading channel.

E. DIVERSTIY AND ERROR CONTROL CODING

As stated, the multipath fading channel is a severe environment in which to communicate. The error rate performance suffers greatly compared to an AWGN channel [9,10,11]. However, two techniques available to mitigate the effects of multipath fading on performance are diversity and error control coding [11]. The possibility exists that a MIMO system can use both of these techniques in order to improve performance [1,13]. In this section, diversity techniques will be investigated. The Alamouti scheme, the focus of the simulations, incorporates diversity techniques in its space–time code, so the performance of diversity techniques is of great interest [1,13].

The concept of diversity is to either transmit and/or receive the same information more than once. If one transmission suffers from a deep fade, then it is possible that other independent faded transmissions will not. The likelihood that all transmissions will be faded below possible recovery is reduced. The receiver, then, can choose from the best receptions [9,10]. There are three methods of diversity: time, frequency and space. Time diversity transmits the same information several times [9,10]. Frequency diversity transmits the same information on several carriers [9,10]. Lastly, space diversity employs several antennas at the receiver in order to receive the same information several times [9,10]. In a MIMO system, multiple antennas are employed so space diversity is possible [1,13]. Also, frequency or time diversity is possible [1,13]. It will be seen that the Alamouti scheme uses both time and space diversity [1,13]. Therefore, the bit error performance of time and space diversity in a multipath fading channel will be considered for BPSK.

1. Maximal-Ratio Combining

The receiver that achieves the best performance in a multipath fading channel is one that uses maximal-ratio combining (MRC). The MRC receiver uses channel estimation, i.e., CSI, of the magnitude and phase of each diversity reception. The MRC receiver multiplies the received diversity reception with the complex conjugate of the estimation. As a consequence, the phase is corrected for coherent detection and the magnitude of the signal is weighted by the signal strength. Strongly received signals will be weighted more than weaker signals (deep faded signals) in the decision process [9,10].

The time diversity reception of one of $l = 1, 2, 3, \ldots L$ diversity signals for a BPSK system is illustrated in Figure 6. Each received diversity signal $r_l(t) = y_l(t) + n_l(t)$ has duration T_c seconds. The correlation receiver equivalent of the matched filter is depicted. Assume that the signal after the correlation receiver is sampled at T_c second intervals. It is then multiplied with the complex conjugate of the CSI represented by $h_l e^{-j\varphi_l}$ associated with that time interval.

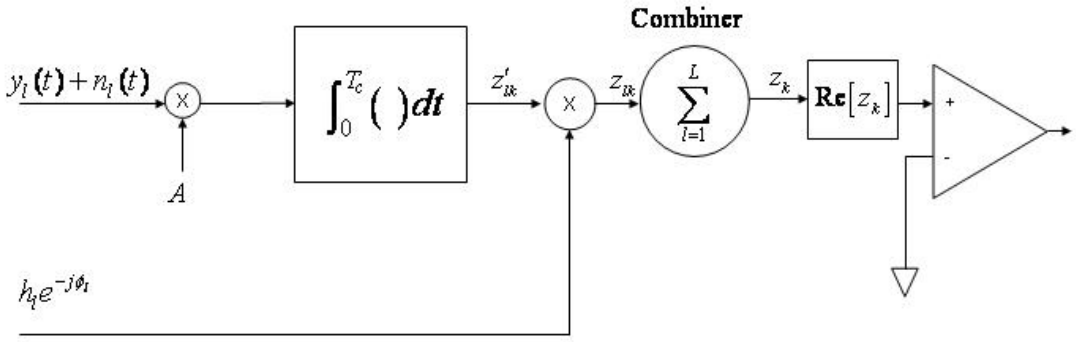

Figure 6. BPSK with time diversity (After Reference [9].).

Let x_k, where $k = 0,1$, be the transmitted baseband BPSK signal defined as

$$\begin{aligned} x_0 &= x_0(t) = Ae^{-j2\pi} = A \qquad \text{for } 0 \le t \le T_c \\ x_1 &= x_1(t) = Ae^{-j\pi} = -A \qquad \text{for } 0 \le t \le T_c. \end{aligned} \tag{2.136}$$

The energy E of a transmitted time diversity signal is [10]

$$E = \int_0^{T_c} |x_0(t)|^2 \, dt = \int_0^{T_c} |x_1(t)|^2 \, dt = A^2 T_c \,. \tag{2.137}$$

As the transmitted signal passes through the multipath fading channel in one time interval T_c seconds, it is multiplied by a channel coefficient $h_l e^{j\varphi_l}$ and AWGN $n_l(t)$ is added. Thus, the received diversity signal $y_l(t)$ in one time interval is given by

$$y_l(t) = h_l e^{j\phi_l} x_k \qquad \text{for } 0 \le t \le T_c \;, \tag{2.138}$$

where l is the time diversity reception and $k = 0,1$.

The symbol z'_{lk} represents the signal after the correlation receiver. The signal is given by

$$\begin{aligned} z'_{lk} &= A\int_0^{T_c} h_l e^{j\varphi_l} x_k + n_l(t)dt \\ &= \begin{cases} A^2 T_c h_l e^{j\varphi_l} + N_l & \text{when } k = 0 \\ -A^2 T_c h_l e^{j\varphi_l} + N_l & \text{when } k = 1, \end{cases} \end{aligned} \tag{2.139}$$

where N_l is

$$N_l = A\int_0^{T_c} n_l(t)\,dt\,. \tag{2.140}$$

Substituting the energy E defined in Equation (2.137) into Equation (2.139), we get

$$z'_{lk} = \begin{cases} Eh_l e^{j\varphi_l} + N_l & \text{when } k = 0 \\ -Eh_l e^{j\varphi_l} + N_l & \text{when } k = 1. \end{cases} \tag{2.141}$$

The signal z_{lk} after multiplication with CSI of the *l*-th reception is given by

$$z_{lk} = \begin{cases} Eh_l^2 + h_l e^{-j\varphi_l} N_l & \text{when } k = 0 \\ -Eh_l^2 + h_l e^{-j\varphi_l} N_l & \text{when } k = 1. \end{cases} \tag{2.142}$$

The symbol z_k represents the signal combined with all L receptions. The signal z_k is given by

$$z_k = \begin{cases} \sum_{l=1}^{L}\left[Eh_l^2 + h_l e^{-j\varphi_l} N_l \right] & \text{when } k = 0 \\ -\sum_{l=1}^{L}\left[Eh_l^2 + h_l e^{-j\varphi_l} N_l \right] & \text{when } k = 1. \end{cases} \tag{2.143}$$

The comparator compares the real part of z_k to zero. If $\mathrm{Re}[z_k] > 0$, a binary 1 is the output. If $\mathrm{Re}[z_k] < 0$, a binary 0 is the output. Then $\mathrm{Re}[z_k]$ is given by

$$\mathrm{Re}[z_k] = \begin{cases} \sum_{l=1}^{L}\left(Eh_l^2 + \mathrm{Re}\left[h_l e^{-j\varphi_l} N_l \right] \right) & \text{when } k = 0 \\ -\sum_{l=1}^{L}\left(Eh_l^2 + \mathrm{Re}\left[h_l e^{-j\varphi_l} N_l \right] \right) & \text{when } k = 1. \end{cases} \tag{2.144}$$

The signal $\mathrm{Re}[z_k]$ is a Gaussian random variable for a fixed set of $\left\{ h_l e^{-j\varphi_l} \right\}$ [10]. The probability of an error P_b is given by [9,10]

$$P_b = Q\left(\frac{\bar{Z}^+}{\sigma_{\mathrm{Re}[z]}} \right), \tag{2.145}$$

where $\overline{Z}^{+}$ is the positive mean of the random variable $\mathrm{Re}[z_k]$, i.e., the expected value of $\mathrm{Re}[z_k]$ when x_0 is transmitted and $\sigma^2_{\mathrm{Re}[z]}$ is the variance of $\mathrm{Re}[z_k]$. The Q-function $Q(x)$ is given by [5]

$$Q(x) = \frac{1}{\sqrt{2\pi}} \int_x^{\infty} e^{-\frac{\xi^2}{2}} d\xi . \tag{2.146}$$

Thus, to find P_b, it is necessary to find $\overline{Z}^{+}$ and $\sigma_{\mathrm{Re}[z]}$. The positive mean $\overline{Z}^{+}$ is given by

$$\begin{aligned} \overline{Z}^{+} &= \sum_{l=1}^{L} E h_l^2 \\ &= E \sum_{l=1}^{L} h_l^2 . \end{aligned} \tag{2.147}$$

The baseband equivalent noise $n_l(t)$ is complex sum of two IID Gaussian noise sources given by

$$n_l(t) = x_l(t) + j y_l(t) . \tag{2.148}$$

The autocorrelation functions of the baseband equivalent noise and its real and imaginary parts are defined as [5]

$$\begin{aligned} R_{nn}(\tau) &= \mathrm{E}\left[n_l^{*}(t)\, n_l(t+\tau) \right] \\ R_{xx}(\tau) &= \mathrm{E}\left[x_l(t)\, x_l(t+\tau) \right] \\ R_{yy}(\tau) &= \mathrm{E}\left[y_l(t)\, y_l(t+\tau) \right]. \end{aligned} \tag{2.149}$$

The power spectral density of the baseband equivalent noise, or its real and imaginary parts, is the Fourier transform of their respective autocorrelation functions. The two–sided baseband equivalent power spectral density $S_{n_l}(f)$ for each diversity reception is defined as [10]

$$S_{n_l}(f) = \begin{cases} N_o & |f| \le \dfrac{B}{2} \\ 0 & |f| > \dfrac{B}{2}, \end{cases} \tag{2.150}$$

where B is an arbitrary bandwidth that is $B \geq 1/T_c$. The power spectral density of the corresponding real bandpass noise $S(f)$ centered about a carrier frequency f_c is [10]

$$S(f) = \begin{cases} \frac{N_o}{4} & |f - f_c| \leq \frac{B}{2} \\ \frac{N_o}{4} & |f + f_c| \leq \frac{B}{2} \\ 0 & \text{otherwise.} \end{cases} \tag{2.151}$$

The variance of the baseband equivalent noise $\sigma_{n_l}^2$ is equal to the total power of the noise given by [5]

$$\sigma_{n_l}^2 = N_o B \,. \tag{2.152}$$

The total power of the baseband equivalent noise is the sum of the real and imaginary parts [5]. Let $\sigma_{nx_l}^2$ represent the variance of the real part and $\sigma_{ny_l}^2$ of the imaginary part. Then the total power of the baseband equivalent noise is given by [5]

$$\sigma_{n_l}^2 = \sigma_{nx_l}^2 + \sigma_{ny_l}^2 \,. \tag{2.153}$$

The real and imaginary parts of the noise are IID with equal variance. Then from Equation (2.153) the variance of the real part $\sigma_{nx_l}^2$ can be derived by

$$\begin{aligned} \sigma_{n_l}^2 &= 2\sigma_{nx_l}^2 \\ 2\sigma_{nx_l}^2 &= N_o B \\ \sigma_{nx_l}^2 &= \frac{N_o B}{2}. \end{aligned} \tag{2.154}$$

Then the power spectral density of the real part of baseband equivalent noise is given by

$$S_{n_x}(f) = \begin{cases} \frac{N_o}{2} & |f| \leq \frac{B}{2} \\ 0 & |f| > \frac{B}{2}. \end{cases} \tag{2.155}$$

The noise power after the matched filter and multiplication by the channel parameter is given by [7,10]

$$\begin{aligned}\sigma_{z_l}{}^2 &= \int_{-\infty}^{\infty} \frac{N_o}{2} \left| h_l^2 e^{-j\varphi} X_0(f) \right|^2 df \\ &= \frac{N_o h_l^2}{2} \int_{-\infty}^{\infty} \left| X_0(f) \right|^2 df .\end{aligned} \tag{2.156}$$

Using Parsevel's theorem in Equation (2.156), we get [5]

$$\begin{aligned}\sigma_{z_l}^2 &= \frac{N_o h_l^2}{2} \int_0^{T_c} \left| x_0(t) \right|^2 dt \\ &= \frac{N_o h_l^2 E}{2} .\end{aligned} \tag{2.157}$$

The variance $\sigma_{\mathrm{Re}[z]}^2$ is the sum of the noise power in each diversity reception and is given by [9]

$$\begin{aligned}\sigma_{\mathrm{Re}[z]}^2 &= \sum_{l=1}^{L} \sigma_{z_l}^2 \\ &= \sum_{l=1}^{L} \frac{N_o h_l^2 E}{2} \\ &= \frac{N_o E}{2} \sum_{l=1}^{L} h_l^2 .\end{aligned} \tag{2.158}$$

Using Equations (2.147) and (2.157) in Equation (2.145), we obtain [9,10]

$$\begin{aligned}P_b &= Q\left(\frac{E \sum_{l=1}^{L} h_l^2}{\sqrt{\frac{N_o E}{2} \sum_{l=1}^{L} h_l^2}} \right) \\ &= Q\left(\sqrt{\frac{2E}{N_o} \sum_{l=1}^{L} h_l^2} \right) .\end{aligned} \tag{2.159}$$

Equation (2.159) is a function of a random variable h_l^2. Let γ be defined as

$$\gamma = \frac{E}{N_0} \sum_{l=1}^{L} h_l^2 . \tag{2.160}$$

Then Equation (2.159) becomes

$$P_b = Q\left(\sqrt{2\gamma} \right) . \tag{2.161}$$

Note that

$$\gamma_l = \frac{Eh_l^2}{N_0} \tag{2.162}$$

represents the instantaneous SNR in the *l*-th reception [10].

In the course of developing the multipath model, the distribution for h_l^2 is already known. If the random variable W_l is defined as

$$W_l = H_l^2, \tag{2.163}$$

then the probability distribution function is

$$f_{W_l}(w_l) = \frac{1}{2\sigma} e^{-w_l/2\sigma^2} u(w_l). \tag{2.164}$$

Note that the average SNR per diversity reception $\overline{\gamma}_l$ is given by

$$\overline{\gamma}_l = \mathrm{E}[\gamma_l] = \mathrm{E}\left[\frac{Eh_l^2}{N_0}\right] = \frac{E}{N_0}\mathrm{E}\left[h_l^2\right] = \frac{E}{N_0}\mathrm{E}[w_l] = \frac{E2\sigma^2}{N_0}. \tag{2.165}$$

The characteristic function of W_l is given by [10]

$$F_{W_l}(\omega) = \frac{1}{(1 - j2\sigma^2\omega)}. \tag{2.166}$$

The probability distribution function of the sum of L IID random variables is the *L*-fold convolution of the original probability distribution, or the multiplication of L characteristic functions [5,10]. If W represents the sum of L random variables W_l, then the characteristic function of *W* is

$$F_W(\omega) = \frac{1}{(1 - j2\sigma^2\omega)^L}. \tag{2.167}$$

This is the characteristic function of the chi-square distribution of degree $2L$. Therefore, the probability distribution function is given by

$$f_W(w) = \frac{w^{L-1}}{2^L \sigma^{2L} \Gamma(L)} e^{-w/2\sigma^2} u(w). \tag{2.168}$$

The parameter L will always be an integer so

$$\Gamma(L) = (L-1)!. \tag{2.169}$$

Then Equation (2.168) becomes

$$f_w(w) = \frac{w^{L-1}}{2^L \sigma^{2L} (L-1)!} e^{-w/2\sigma^2} u(w). \tag{2.170}$$

Transforming this distribution with

$$\Gamma = \frac{E}{N_0} W, \tag{2.171}$$

where

$$\frac{d\gamma}{dw} = \frac{E}{N_o}, \tag{2.172}$$

we get

$$f_\Gamma(\gamma) = \frac{1}{\frac{E}{N_0}} \frac{w^{L-1}}{2^L \sigma^{2L} (L-1)!} e^{-w/2\sigma^2} \Bigg|_{w=\frac{\gamma}{E/N_o}}. \tag{2.173}$$

Equation (2.173) becomes

$$f_\Gamma(\gamma) = \frac{\gamma^{L-1}}{\left(\frac{E2\sigma^2}{N_0}\right)^L (L-1)!} e^{-\frac{\gamma}{\frac{E2\sigma^2}{N_o}}}. \tag{2.174}$$

Substituting the average SNR $\overline{\gamma}_l$, Equation (2.165), into Equation (2.174), we obtain

$$f_\Gamma(\gamma) = \frac{\gamma^{L-1}}{(\overline{\gamma})^L (L-1)!} e^{-\frac{\gamma}{\overline{\gamma}_l}} u(\gamma). \tag{2.175}$$

Equation (2.175) is the probability distribution function for Γ as a function of γ. The probability of bit error is also written as a function of γ. The average probability of bit error in a multipath fading channel can be derived by taking the expectation of the bit error probability, that is [9,10],

$$\begin{aligned}\overline{P_e} &= \mathrm{E}\left[P_b(\gamma)\right] \\ &= \int_{-\infty}^{\infty} P_b(\gamma) f_\Gamma(\gamma) d\gamma.\end{aligned} \tag{2.176}$$

Substituting Equations (2.161) and (2.175) into (2.176), we get

$$\overline{P_e} = \int_0^\infty Q\left(\sqrt{2\gamma}\right) \frac{\gamma^{L-1}}{\left(\overline{\gamma}_l\right)^L (L-1)!} e^{-\frac{\gamma}{\overline{\gamma}_l}} d\gamma\,. \tag{2.177}$$

This has a solution given by [10]

$$\overline{P_e} = \left[\frac{(1-u)}{2}\right]^L \sum_{l=0}^{L-1} \binom{L-1+l}{l} \left[\frac{(1+u)}{2}\right]^l, \tag{2.178}$$

where the parameter u is given by

$$u = \sqrt{\frac{\overline{\gamma}}{1+\overline{\gamma}}}\,. \tag{2.179}$$

In time–diversity, the combiner adds L diversity receptions in succession. The transmit interval T_c is related to the bit duration T_b by [9]

$$T_b = LT_c\,. \tag{2.180}$$

Let the energy per bit E_b be defined as

$$E_b = A^2 T_b\,. \tag{2.181}$$

The correlation filter of the MRC integrates over one diversity reception T_c. The energy per bit relates to energy per reception by [9]

$$E_b = LE\,, \tag{2.182}$$

or

$$E = \frac{E_b}{L}\,. \tag{2.183}$$

Substituting Equation (2.183) into Equation (2.165), we get

$$\overline{\gamma}_l = \frac{E_b 2\sigma^2}{LN_0}. \tag{2.184}$$

In space–diversity, the MRC is configured as in Figure 7. The space–diversity receptions come from separate receivers, and the time interval T of the matched filter is one bit period T_b, i.e., $T_b = T$. Therefore, the energy per diversity reception is equal to the energy per bit

$$E = E_b. \tag{2.185}$$

The average SNR per reception becomes

$$\overline{\gamma}_l = \frac{E_b 2\sigma^2}{N_o}. \tag{2.186}$$

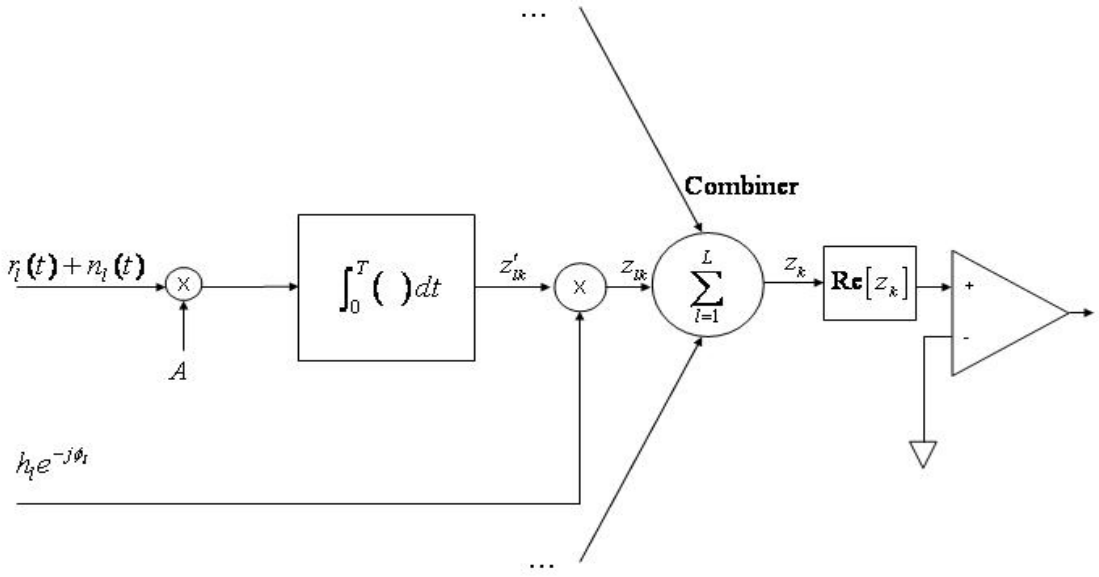

Figure 7. MRC space diversity configuration (After Reference [9].).

Of special interest is when $L=1$, i.e., no diversity. The average SNR per reception for both time and space diversity schemes reduces to

$$\overline{\gamma}_l = \frac{E_b 2\sigma^2}{N_o}. \tag{2.187}$$

The probability of bit error $\overline{P_e}$ reduces to

$$\overline{P_e} = \left[\frac{(1-u)}{2}\right]. \tag{2.188}$$

Substituting Equation (2.179) into Equation (2.188), we obtain

$$\overline{P_e} = \left[\frac{1}{2}\left(1-\sqrt{\frac{\overline{\gamma}_l}{1+\overline{\gamma}_l}}\right)\right]. \tag{2.189}$$

This result is the probability of bit error $\overline{P_e}$ for a BPSK SISO system in a multipath fading channel [9,10]. Equation (2.189) will be the benchmark for simulations in a multipath fading environment. Furthermore, the means to analyze an MRC receiver is obtained. This will be essential in the analysis of the design.

F. SPACE-TIME CODING

"An effective and practical way to approaching the capacity of MIMO wireless channels is to employ space–time coding" [1]. Space–time coding is simply transmitting signals over the channel from multiple antennas to multiple antennas in such a way that capacity is maximized. Maximum capacity can only be approached. Space–time codes are designed to achieve both time and space diversity to improve the error performance and achieve diversity gain [1].

Another mechanism to improve performance is error control coding (ECC) [1]. Error control coding arranges the transmitted symbols in such a way as to increase immunity to noise. It is realized by introducing redundant bits to the information bit stream, allowing the receiver to detect and possibly correct errors. However, increasing the number of bits in the bit stream increases the bandwidth required to transmit the information [10,11]. If the error control coding is designed in conjunction with the modulation

technique and the transmit diversity scheme, then it is possible that there is no bandwidth expansion. With ECC, coding gain is achieved [1].

Overall, it is possible to achieve both diversity and coding gain with space–time codes [1]. (The general effects of diversity and coding on performance are illustrated in Figure 8 from Reference [13].). In general it depicts the possibility of improving performance by the introduction of diversity and ECC. The focus of this thesis is diversity gain; the addition of error control coding is left for future work.

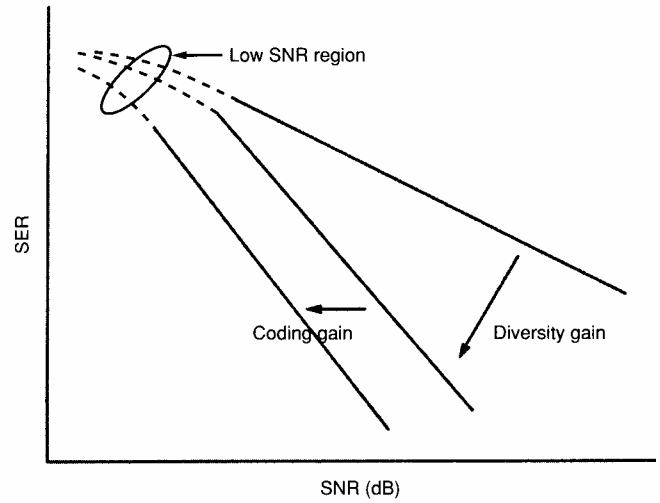

Figure 8. Diversity and coding gain (From Reference [13].).

In this chapter, the fundamentals necessary to understand a MIMO system in a multipath fading environment were introduced. It was seen that the capacity of a MIMO system can increase linearly with the number of transmit and receive antennas. To approach this capacity, space–time codes are designed to incorporate diversity and error control techniques. A baseband model of a slow fading, frequency nonselective multipath fading channel was obtained for simulation. Lastly, diversity techniques with the MRC receiver were examined to facilitate analysis of the design. In the next chapter, the Alamouti space–time coding scheme is introduced, and a transmitter and receiver design will be developed.

THIS PAGE INTENTIONALLY LEFT BLANK

III. MULTIPLE–INPUT–MULTIPLE–OUTPUT TRANSMITTER AND RECEIVER USING THE ALAMOUTI SPACE–TIME CODING SCHEME

This chapter introduces the Alamouti space–time code. Once the code is presented, it will be used to design the MIMO transmitter and receiver using BPSK modulation. The designs will be simulated in Chapter IV and bit error performance will be analyzed and tested.

A. THE ALAMOUTI SPACE–TIME CODING SCHEME

The Alamouti space–time scheme was introduced in Reference [14]. It is a space–time code for transmission through two antennas, $N_t = 2$. It will be used in a MIMO configuration with two receive antennas, $N_r = 2$.

To describe signals more precisely from transmitter to receiver, the following notation will be adhered to through the remainder of this thesis. Let:

- x_n^m represents the signal x in the *n*-th transmission interval from the *m*-th antenna,
- $\boldsymbol{x}^m$ represents the signal over the complete code sequence from the m-th antenna,
- square brackets $[\ ]$ encompass the total space–time code. The elements within the brackets separated by commas represent the code signal of one time interval, and
- asterisk * represents the complex conjugate of the signal.

Let x_1 and x_2 represent the baseband equivalent of signals for BPSK modulated bits over two consecutive transmission intervals of T seconds. Each is represented by $\pm A$. Let $\boldsymbol{x}^1$ and $\boldsymbol{x}^2$ be the Alamouti space–time coded signals transmitted from antenna one and antenna two, respectively. Then the Alamouti space–time coded signals are defined by [1,13]

$$\begin{aligned} \boldsymbol{x}^1 &= \left[x_1, -x_2^* \right] \\ \boldsymbol{x}^2 &= \left[x_2, x_1^* \right]. \end{aligned} \tag{3.1}$$

Although x_1 and x_2 are real in this case, the complex conjugate remains for generality and possible transformation to complex values in future work.

The Alamouti space–time code, as it emanates from either antenna, contains information necessary to demodulate successive information bits. The combination of the two consecutive signals from both transmit antennas corresponds to time diversity. Two antennas are used at the receiver, thus, space diversity is also achieved [1].

The Alamouti scheme has two important features [1]. First, the coded signals from the two transmit antennas are orthogonal over the code interval. If $\boldsymbol{x}^1$ and $\boldsymbol{x}^2$ are considered as complex vectors then they are orthogonal if their inner product equals zero [4,6]. Specifically,

$$\boldsymbol{x}^1 \left(\boldsymbol{x}^2 \right)^{*T} = 0 . \tag{3.2}$$

Expansion of left hand side of Equation (3.2) gives

$$\begin{aligned} \boldsymbol{x}^1 \left(\boldsymbol{x}^2 \right)^{*T} &= \left[x_1 - x_2^* \right] \begin{bmatrix} x_2^* \\ x_1 \end{bmatrix} \\ &= x_1 x_2^* - x_1 x_2^* = 0. \end{aligned} \tag{3.3}$$

Thus, $\boldsymbol{x}^1$ and $\boldsymbol{x}^2$ are orthogonal.

To describe the second feature, first let the code matrix be defined by $\mathbf{X}$. The code matrix $\mathbf{X}$ is the combination of $\boldsymbol{x}^1$ and $\boldsymbol{x}^2$ and is given by [1]

$$\mathbf{X} = \begin{bmatrix} \boldsymbol{x}^1 \\ \boldsymbol{x}^2 \end{bmatrix} = \begin{bmatrix} x_1 & -x_2^* \\ x_2 & x_1^* \end{bmatrix}. \tag{3.4}$$

Then, $\mathbf{X}\mathbf{X}^{*T}$ is

$$\begin{aligned}\mathbf{X}\mathbf{X}^{*T} &= \begin{bmatrix} x_1 & -x_2^* \\ x_2 & x_1^* \end{bmatrix}\begin{bmatrix} x_1^* & x_2^* \\ -x_2 & x_1 \end{bmatrix} \\ &= \begin{bmatrix} x_1x_1^* + x_2x_2^* & x_1x_2^* - x_2^*x_1 \\ x_2x_1^* - x_1^*x_2 & x_2x_2^* + x_1^*x_1 \end{bmatrix} \\ &= \begin{bmatrix} |x_1|^2 + |x_2|^2 & 0 \\ 0 & |x_1|^2 + |x_2|^2 \end{bmatrix} \\ &= \left(|x_1|^2 + |x_2|^2\right)\mathbf{I}_2.\end{aligned} \tag{3.5}$$

Equation (3.5) represents a scalar multiplied by an identity matrix. Note as well that the orthogonal feature of the Alamouti code is encompassed in this feature. Furthermore, this feature represents a condition similar to the example of the capacity of MIMO systems in Chapter II. It was found that with this matrix, i.e., a scalar multiplied by the identity matrix, the capacity increased linearly with the rank of $\mathbf{H}$. This feature and its importance will become clear in the next chapter.

With the Alamouti space–time coding scheme defined, the transmitter and receiver can now be designed. A generic transmitter and receiver is described in Reference [1]. The transmitter and receiver described next is the implementation using BPSK modulation.

B. TRANSMITER

The objective of the transmitter is clear; produce two BPSK signals from an information bit stream for transmission from two transmit antennas according to Equation (3.1). The transmitter design is shown in Figure 9. Let the binary information source be represented by b. The binary information source undergoes serial-to-parallel conversion to produce two binary bits b_1 and b_2 in successive intervals. Next, the two binary symbols are modulated by baseband BPSK modulators to give the corresponding two baseband equivalent signals x_1 and x_2. In turn, x_1, x_2 and their complex conjugates are routed to two parallel-to-serial converters to produce $\boldsymbol{x}^1$ and $\boldsymbol{x}^2$ as defined by Equation (3.1).

An important feature of the transmitter is that the transmission rate of the information source R_b is equal to the transmission rate of each of the two transmitted signals $\boldsymbol{x}^1$ and $\boldsymbol{x}^2$. Each bit period is T seconds and is equal to the original bit period. The serial-to-parallel and parallel-to-serial conversion combination maintains the transmission rate of the binary information source R_b. This is another important feature of space–time coding. In MIMO systems, time and space diversity can be achieved without bandwidth expansion[1]. In this case, the Alamouti space–time code achieves both space and time diversity while maintaining the original transmission rate R_b through the channel.

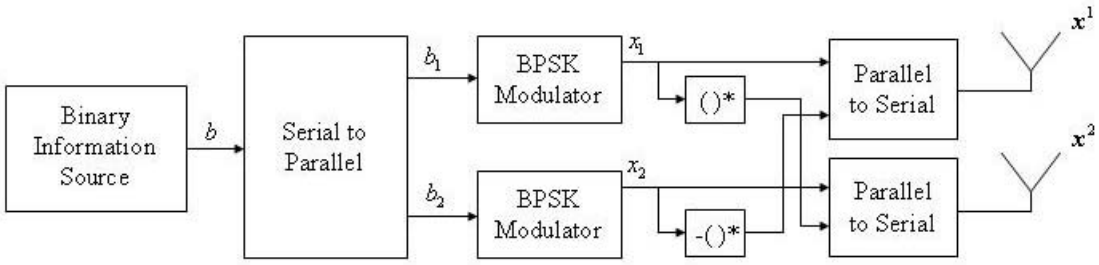

Figure 9. MIMO Transmitter.

C. RECEIVER

The transmitter was relatively straightforward to design. The receiver is somewhat more complicated. Let the signal available at each receive antenna be the represented by $\boldsymbol{r}^1$ and $\boldsymbol{r}^2$. In the absence of AWGN and multipath fading (i.e., all channel coefficients equal one), $\boldsymbol{r}^1$ and $\boldsymbol{r}^2$ are given by

$$\begin{aligned} \boldsymbol{r}^1 &= \boldsymbol{x}^1 + \boldsymbol{x}^2 \\ \boldsymbol{r}^2 &= \boldsymbol{x}^1 + \boldsymbol{x}^2. \end{aligned} \tag{3.6}$$

Incorporation of the definitions for $\boldsymbol{x}^1$ and $\boldsymbol{x}^2$ from Equation (3.1) into Equation (3.6) gives

$$\begin{aligned} \boldsymbol{r}^1 &= \left[x_1, -x_2^* \right] + \left[x_2, x_1^* \right] \\ \boldsymbol{r}^2 &= \left[x_1, -x_2^* \right] + \left[x_2, x_1^* \right]. \end{aligned} \tag{3.7}$$

Over the code sequence the same information is available at each receive antenna. This is possible because of the assumption that all channel coefficients are equal to one. In a fading environment this will not be the case. Nevertheless, there is time and space diversity capability, an advantage that should be exploited. The logic of the receiver design is to exploit this and maximize the diversity reception of x_1 and x_2.

Let the signals be isolated in one transmission interval *T*. A serial-to-parallel converter performs this function. The received signals by transmission interval are

$$\boldsymbol{r}^1 = \left[r_1^1, r_2^1 \right] = \left[x_1 + x_2, x_1^* - x_2^* \right], \tag{3.8}$$

and

$$\boldsymbol{r}^2 = \left[r_1^2, r_2^2 \right] = \left[x_1 + x_2, x_1^* - x_2^* \right]. \tag{3.9}$$

If the complex conjugate is taken on r_2^1 and r_2^2, the received signals become

$$\begin{aligned} r_1^1 &= x_1 + x_2 \\ \left(r_2^1 \right)^* &= x_1 - x_2, \end{aligned} \tag{3.10}$$

and

$$\begin{aligned} r_1^2 &= x_1 + x_2 \\ \left(r_2^2 \right)^* &= x_1 - x_2. \end{aligned} \tag{3.11}$$

From a closer look at Equations (3.10) and (3.11), there is a total of four signals available. The signals in each time interval, distinguished with different subscripts, represent time diversity signals. The signals received by each antenna, distinguished by different superscripts, represent space diversity signals. By combining correctly, both x_1 and x_2 can be isolated. Let z_1^m and z_2^m, where $m = 1, 2$, be the time diversity combination on the *m*-th space diversity reception that isolates x_1 and x_2 respectively. Then the time diversity combination for x_1 is given by

$$\begin{aligned} z_1^m &= r_1^m + \left(r_2^m\right)^* \\ &= x_1 + x_2 + x_1 - x_2 \\ &= 2x_1. \end{aligned} \tag{3.12}$$

Similarly, the time diversity combination for x_2 is given by

$$\begin{aligned} z_2^m &= \boldsymbol{r}_1^m - \left(\boldsymbol{r}_2^m\right)^* \\ &= x_1 + x_2 - \left(x_1 - x_2\right) \\ &= 2x_2. \end{aligned} \tag{3.13}$$

Both time diversity combinations are available on both space diversity receptions. By combining these correctly, x_1 and x_2 can be further emphasized. Let z_1 and z_2 be the space diversity combinations that result in x_1 and x_2, respectively. Then, z_1 is given by

$$\begin{aligned} z_1 &= z_1^1 + z_1^2 \\ &= 2x_1 + 2x_1 \\ &= 4x_1, \end{aligned} \tag{3.14}$$

and z_2 is given by

$$\begin{aligned} z_2 &= z_2^1 + z_2^2 \\ &= 2x_2 + 2x_2 \\ &= 4x_2. \end{aligned} \tag{3.15}$$

From the logic of Equations (3.12) through (3.15), it is possible to build a receiver to take advantage of both time and space diversity receptions and isolate x_1 and x_2.

Lastly, the signals z_1 and z_2 need only be demodulated to produce $\hat{b}_1$ and $\hat{b}_2$, where the '^' distinguishes the demodulated binary signal from the original signal. Lastly, $\hat{b}_1$ and $\hat{b}_2$ are sent to a parallel-to-serial converter to reproduce the demodulated information bit stream $\hat{b}$. The receiver design is illustrated in Figure 10.

The MIMO system that features the Alamouti space–time code is now designed. The system incorporates transmit and space diversity techniques in order to combat the effects of the multipath fading channel. In the next chapter, the design is implemented in

Matlab with Simulink and is tested for performance with AWGN alone and AWGN in a multipath fading environment.

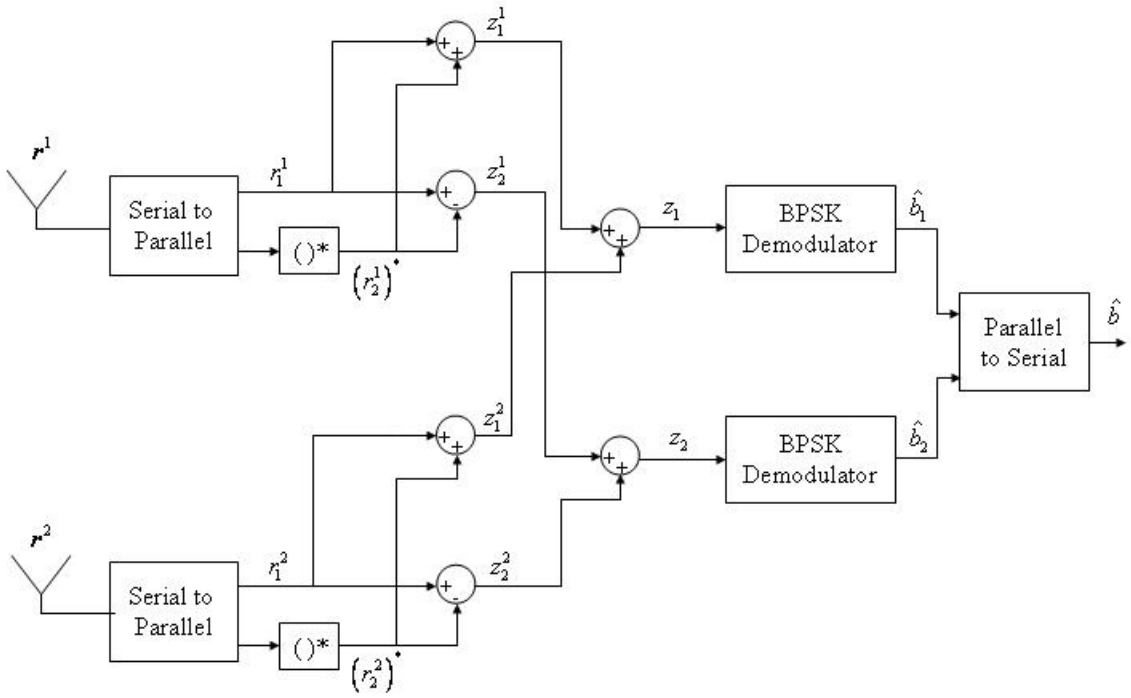

Figure 10. MIMO Receiver.

THIS PAGE INTENTIONALLY LEFT BLANK

IV. ANALYSIS AND SIMULATION

In this chapter the error performance analysis and simulation of the MIMO system with the Alamouti space–time code is presented. The system, as described in Chapter III, was simulated in Matlab using Simulink. The system is analyzed and simulated in a progressive manner from an AWGN channel to the multipath fading channel. To facilitate a smooth transition from each progressive step, the changes to the original simulation setup are highlighted. The simulation of the transmitter and receiver are described first.

For ease of presentation, the Matlab simulation blocks, as they are used in the simulations, are presented in Appendix B. Further information concerning the blocks and the parameters are found in Reference [15]. The parameters, as depicted in Appendix B, are maintained throughout all simulations.

Each simulation is compared to a baseband equivalent SISO BPSK system. An important parameter for comparison is the average energy per bit E_b. In a single channel BPSK system, E_b is equal if a binary bit zero or one is transmitted. Let the modulated signal for a binary zero be represented by $x_0(t)$. If the amplitude over a period of T seconds is represented by A, then E_b is given by [10]

$$E_b = \int_0^T \left| x_0(t) \right|^2 dt = A^2 T . \tag{4.1}$$

The energy per bit is referenced to the output of the transmitter, thus the transmitted power into the channel for the SISO system is defined by

$$P_{SISO} = \frac{E_b}{T} . \tag{4.2}$$

The symbol E_s is defined as the energy per symbol and is used to represent the energy per symbol period of the MIMO system. This is done in order to distinguish between the energies of the SISO and MIMO systems. The mathematical representation of E_s will be derived later in this chapter. It will also be referenced to the output of the transmitter, and the transmitted power into the channel for one MIMO antenna is defined by

$$P_{MIMO} = \frac{E_s}{T}. \tag{4.3}$$

A. SIMULATION OF THE MIMO TRANSMITTER AND RECEIVER

1. MIMO Transmitter Simulation

The block diagram of the transmitter simulation is given in Figure 11. The transmitter information source is a Bernoulli binary generator block. It produces the binary information source b. The output is a binary bit stream of 1s and 0s according to three parameters. The first is the probability of zero. Since the ones and zeros are equally likely, this parameter is set to 0.5. The second parameter is the initial seed for the random number generator. This value is a prime number that must be different from all other random sources in the simulation. By ensuring different seeds, the statistical independence of all sources is simulated [15]. The last parameter is sample time, which is set at the value T [15].

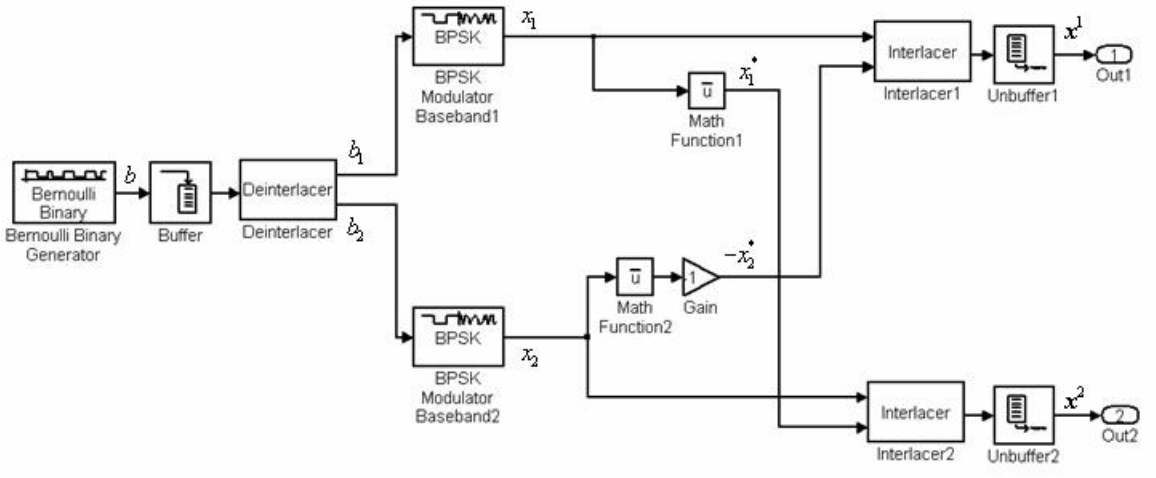

Figure 11. MIMO Transmitter Simulation.

The next two blocks in the MIMO transmitter are the buffer and deinterlacer. The buffer takes the input bit sequence *b* and produces a 2-by-1 frame at a sample time of $2T$ seconds. The deinterlacer splits the frame into two separate outputs, isolating b_1 and

b_2 for manipulation. Together, the buffer and deinterlacer provide the serial-to-parallel conversion of the bit stream. The buffer must wait for $2T$ seconds before producing an output that was generated by the Bernoulli binary generator. This causes a delay of $2T$ seconds.

Now that b_1 and b_2 are separated, each is sent to a baseband equivalent BPSK modulator to produce the modulated symbols x_1 and x_2. The modulation of the binary data is accomplished according to Table 1.

Input $b_{1,2}$	Output $x_{1,2}$
0	A
1	$-A$

Table 1. Modulation of binary data.

where the amplitude $A = 1$. The modulated signal x_1 is routed through a complex conjugate block to produce x_1^*. Similarly, x_2 is routed through a complex conjugate block and a negative gain block to produce $-x_2^*$. The baseband modulated symbols x_1, x_1^*, x_2 and $-x_2^*$ are then routed to the input of two interlacer blocks to form the final outputs. The interlacer and unbuffer blocks provide the parallel-to-serial conversion. The output of each unbuffer block has a period of T seconds. The output identified in Figure 11 as "Out1" is the code sequence for antenna 1, $\boldsymbol{x}^1$. Likewise, the "Out2" is the code sequence for antenna 2, $\boldsymbol{x}^2$. Each conforms to the required code sequence of the Alamouti space–time code given in Chapter III.

2. MIMO Receiver Simulation

The block diagram of the receiver simulation is shown in Figure 12. The inputs indicated in the figure as "In1" and "In2" represent the received signals from antennas 1 and 2, respectively, that is $\boldsymbol{r}^1$ and $\boldsymbol{r}^2$. The buffer and deinterlacer blocks are identical to

the transmitter and serve as the serial-to-parallel conversion of the received signals $\boldsymbol{r}^1$ and $\boldsymbol{r}^2$. However, it is important to note, as with the transmitter, the buffer blocks introduce another delay of $2T$. The total delay through the system is now $4T$. The math function blocks implement the complex conjugate of their respective inputs. The summing blocks are the time and space diversity combining described in Chapter III.

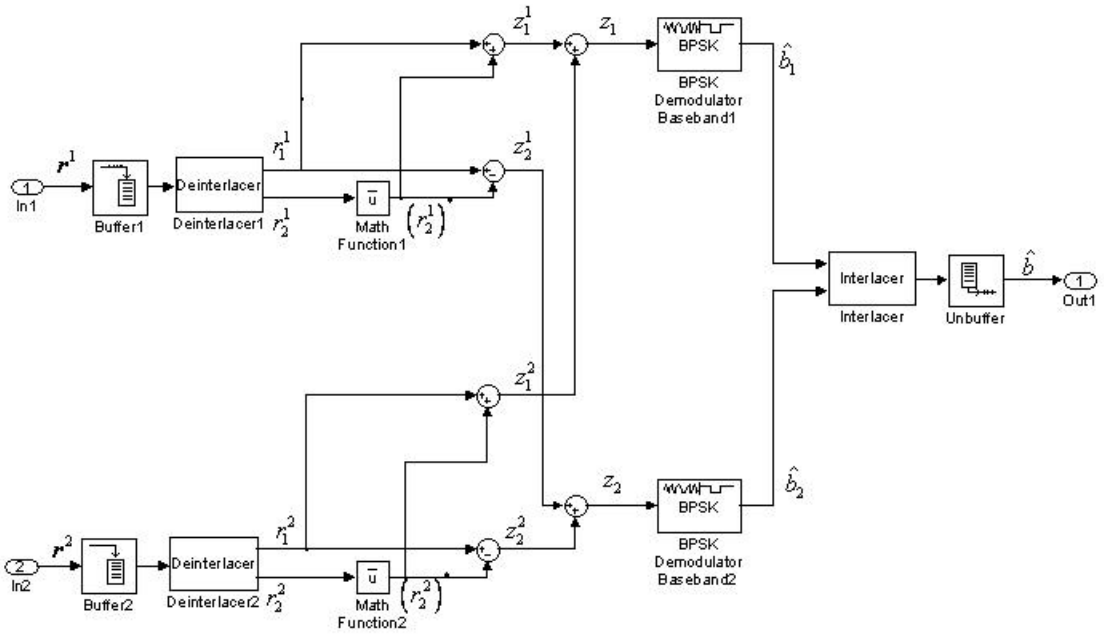

Figure 12. MIMO Receiver Simulation.

The baseband equivalent demodulator blocks demodulate the incoming signals according to Table 2 [15].

Input $z_{1,2}$	Output $\hat{b}_{1,2}$
$\mathrm{Re}\left[z_{1,2}\right] \geq 0$	0
$\mathrm{Re}\left[z_{1,2}\right] < 0$	1

Table 2. Demodulation to binary data.

The output of the two demodulator blocks are the binary bit streams $\hat{b}_1$ and $\hat{b}_2$. The final two blocks, the interlacer and unbuffer, serve as the parallel-to-serial converter producing the demodulated binary information $\hat{b}$.

B. SIMULATION IN AWGN

The MIMO system is first subjected to AWGN only. In this simulation, it is assumed there is no fading. This implies that the channel coefficients h_{ij} are all constant and equal to one. A block diagram of the MIMO system in AWGN is illustrated in Figure 13. Both the MIMO transmitter and receiver are collapsed into subsystems for ease of presentation. They remain the same as those described in Figure 11 and Figure 12, respectively. In this simulation, two gain blocks are introduced at the outputs of the transmitter. This is done to normalize the total power transmitted into the channel for comparison to a SISO BPSK system. The MIMO channel in AWGN consists of the output of the two gain blocks to the two inputs of the MIMO receiver. The two AWGN channel blocks are complex white Gaussian noise sources that add to the incoming signals. They are represented by $\boldsymbol{n}^1$ and $\boldsymbol{n}^2$.

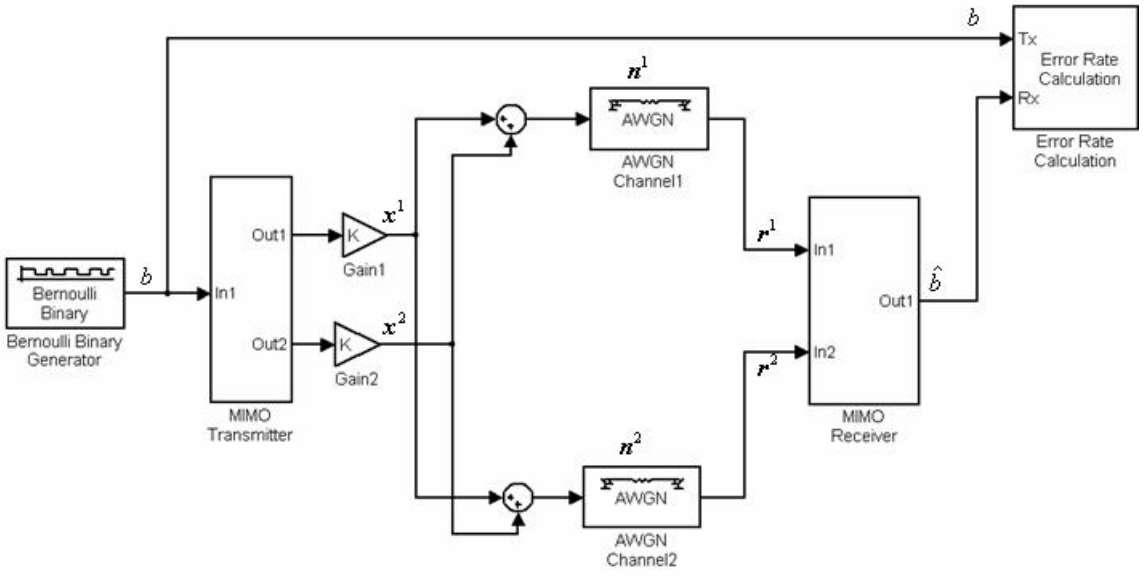

Figure 13. Simulation in AWGN.

1. Simulation Parameters

The factor K in the gain blocks is determined from the discussion of the MIMO model in Chapter II. The power emanating from both of the transmit antennas is equal. Let the power from any antenna be represented by P^{Ant}. Let the total power transmitted into the channel be represented by P. The power from any antenna is the total power divided by the number of transmit antennas, in this case $N_t = 2$. The power from any antenna P^{Ant} is given by

$$P^{Ant} = \frac{P}{N_t} = \frac{P}{2}. \tag{4.4}$$

The energy E_s in any symbol x_1, x_2 x_1^* or x_2^* is equal whether a binary zero or one is transmitted. The distinction between the SISO and MIMO system is the MIMO system symbols include the multiplication of K by the gain blocks. Once again, let the modulated signal for a binary zero be represented by $x_0(t)$. If the amplitude over a period of T seconds is represented by A, then E_s is given by [10]

$$E_s = \int_0^T \left| K x_0(t) \right|^2 dt = \int_0^T K^2 A^2 dt = K^2 A^2 T. \tag{4.5}$$

The power emitted by each antenna is equal to the symbol power given by [7]

$$P^{Ant} = \frac{E_s}{T} = K^2 A^2. \tag{4.6}$$

When Equations (4.4) and (4.6) are equated, the total signal power into the channel as a function of amplitude and the gain factor K is given as

$$\begin{aligned} \frac{P}{2} &= K^2 A^2 \\ P &= 2K^2 A^2. \end{aligned} \tag{4.7}$$

The total power at the input of either of the AWGN blocks with no fading is also given by P. This is set to 1.0 Watt. The amplitude A is 1.0 Volt. Using this information in Equation (4.7), we obtain

$$K^2 = \frac{1}{2}$$
$$K = \frac{1}{\sqrt{2}}. \tag{4.8}$$

Thus, the gain factor K is set to $1/\sqrt{2}$ in this and all subsequent simulations. The energy per symbol E_s of the MIMO system is

$$E_s = \frac{A^2 T}{2}. \tag{4.9}$$

The energy per symbol for x_1, x_2, x_1^* or x_2^* is given by Equation (4.9). It incorporates the gain factor K. Thus, if a bit zero is transmitted in the MIMO system, represented by $x_0(t)$, it is given by

$$x_0(t) = \frac{A}{\sqrt{2}} \quad \text{for } 0 \le t \le T. \tag{4.10}$$

Comparing the energy per bit E_b of the SISO system, Equation (4.1), and the energy per symbol E_s of the MIMO system, Equation (4.9), we have

$$E_s = \frac{E_b}{2}. \tag{4.11}$$

The AWGN channel blocks require several parameters: an initial seed, the energy per symbol–to–noise ratio E_s/N_o, the power of the input signal, and the symbol period. The symbol period is set to T seconds. The average energy per symbol–to–noise ratio E_s/N_o increases with each simulation run. The initial seed is a prime number that is different in each block as well as different from the initial seed of the Bernoulli binary generator block.

Finally, the error rate calculation block compares each bit from the original bit stream b with the demodulated bit stream $\hat{b}$ over the simulation run. It calculates the bit error rate or simulated probability of bit error. The total delay of $4T$ is incorporated in this block to ensure that the comparison of b and $\hat{b}$ is synchronized in time.

2. Performance Analysis

At each receive antenna, the received signals $\boldsymbol{r}^1$ and $\boldsymbol{r}^2$ are given by

$$\begin{aligned} \boldsymbol{r}^1 &= \left(\boldsymbol{x}^1 + \boldsymbol{x}^2\right) + \boldsymbol{n}^1 \\ \boldsymbol{r}^2 &= \left(\boldsymbol{x}^1 + \boldsymbol{x}^2\right) + \boldsymbol{n}^2. \end{aligned} \tag{4.12}$$

The complex valued vectors $\boldsymbol{n}^1$ and $\boldsymbol{n}^2$ in Equation (4.12) represent the noise over two consecutive bits added at receive antennas 1 and 2, respectively. If the definitions for $\boldsymbol{x}^1$ and $\boldsymbol{x}^2$ from Chapter III are incorporated, then Equation (4.12) becomes

$$\begin{aligned} \boldsymbol{r}^1 &= \left(\left[x_1, -x_2^*\right] + \left[x_2, x_1^*\right]\right) + \left[n_1^1, n_2^1\right] \\ \boldsymbol{r}^2 &= \left(\left[x_1, -x_2^*\right] + \left[x_2, x_1^*\right]\right) + \left[n_1^2, n_2^2\right]. \end{aligned} \tag{4.13}$$

After serial-to-parallel conversion, the signals in each time and space diversity reception are given by

$$\boldsymbol{r}^1 = \left[r_1^1, r_2^1\right] = \left[\left(x_1 + x_2\right) + n_1^1, \left(x_1^* - x_2^*\right) + n_2^1\right], \tag{4.14}$$

and

$$r^2 = \left[r_1^2, r_2^2\right] = \left[\left(x_1 + x_2\right) + n_1^2, \left(x_1^* - x_2^*\right) + n_2^2\right]. \tag{4.15}$$

The time diversity combination of the received signal on antenna 1, represented by z_1^1 and z_2^1, respectively, are

$$\begin{aligned} z_1^1 &= r_1^1 + \left(r_2^1\right)^* \\ &= \left(x_1 + x_2\right) + n_1^1 + \left(\left(x_1^* - x_2^*\right) + n_2^1\right)^* \\ &= 2x_1 + n_1^1 + n_2^{1*}, \end{aligned} \tag{4.16}$$

and

$$\begin{aligned} z_2^1 &= r_1^1 - \left(r_2^1\right)^* \\ &= \left(x_1 + x_2\right) + n_1^1 - \left(\left(x_1^* - x_2^*\right) + n_2^1\right)^* \\ &= 2x_2 + n_1^1 - n_2^{1*}. \end{aligned} \tag{4.17}$$

Similarly, the time diversity combination of the received signal on antenna 2, z_1^2 and z_2^2, are

$$\begin{aligned} z_1^2 &= 2x_1 + n_1^2 + n_2^{2*} \\ z_2^2 &= 2x_2 + n_1^2 - n_2^{2*}. \end{aligned} \tag{4.18}$$

The space diversity combining of x_1 and x_2 are represented by z_1 and z_2. After space diversity combining, z_1 is

$$\begin{aligned} z_1 &= z_1^1 + z_1^2 \\ &= 2x_1 + n_1^1 + n_2^{1*} + 2x_1 + n_1^2 + n_2^{2*} \\ &= 4x_1 + n_1^1 + n_2^{1*} + n_1^2 + n_2^{2*}, \end{aligned} \tag{4.19}$$

and z_2 is

$$\begin{aligned} z_2 &= z_2^1 + z_2^2 \\ &= 2x_2 + n_1^1 - n_2^{1*} + 2x_2 + n_1^2 - n_2^{2*} \\ &= 4x_2 + n_1^1 - n_2^{1*} + n_1^2 - n_2^{2*}. \end{aligned} \tag{4.20}$$

It is important to note the symmetry of the receiver. In Equations (4.19) and (4.20), x_1 and x_2 are the BPSK baseband modulation of two binary random variables that are IID. The noise components n_1^1, n_2^{1*}, n_1^2 and n_2^{2*} represent zero-mean IID complex Gaussian random variables. The sum of the means is zero, and the sum of variances is equal in both Equations (4.19) and (4.20) [5]. Thus, the probability of error in demodulating z_1 and z_2 are equal. The overall probability of bit error of the system is the average of the two. Since they are equal, the probability of bit error of the system is the probability of error in demodulating either z_1 or z_2.

Let the overall probability of bit error be represented by P_e. To determine P_e, z_1 is used. The demodulator takes the real part of z_1. Let z be the real part of z_1, given by

$$\begin{aligned} z &= \mathrm{Re}(z_1) = \mathrm{Re}\left(4x_1 + n_1^1 + n_2^{1*} + n_1^2 + n_2^{2*}\right) \\ &= 4x_1 + \mathrm{Re}\left(n_1^1\right) + \mathrm{Re}\left(n_2^{1*}\right) + \mathrm{Re}\left(n_1^2\right) - \mathrm{Re}\left(n_2^{2*}\right). \end{aligned} \tag{4.21}$$

Let the sum of the real parts of all the noise components be represented by n. Then Equation (4.21) reduces to

$$z = 4x_1 + n. \tag{4.22}$$

Equation (4.22) defines a Gaussian random variable Z. The probability of bit error for a Gaussian random variable P_e [9,10] is

$$P_e = Q\left(\frac{\bar{Z}^+}{\sigma_z}\right), \tag{4.23}$$

where $\bar{Z}^+$ is the positive mean of Z (i.e., the mean of Z when a binary 0 is transmitted). Let $x_0(t)$ represent the modulated signal x_1 when a binary 0 is transmitted. If matched filter conditions are assumed, then the positive mean $\bar{Z}^+$ at the output of the receiver is given by [9,10]

$$\begin{aligned} \bar{Z}^+ &= 4\int_0^T x_0(t)\,x_0(t)dt \\ &= 4\int_0^T x_0^2(t)dt \\ &= 4E_s. \end{aligned} \tag{4.24}$$

The power spectral density of the real part of each noise component is $N_o/2$ Watts per Hertz [15]. Let the total noise power of the real part of the noise be represented by σ_o^2. The noise power σ_o^2 for each noise component after the matched filter is

$$\sigma_o{}^2 = \int_{-\infty}^{\infty} \frac{N_o}{2}\left|X_0(f)\right|^2 df. \tag{4.25}$$

By Parsevel's theorem [5], Equation (4.25) converts to

$$\begin{aligned} \sigma_o{}^2 &= \int_0^T \frac{N_o}{2}\left|x_0(t)\right|^2 dt \\ &= \frac{N_o E_s}{4}. \end{aligned} \tag{4.26}$$

Let the total noise power of Z be represented by σ_z^2. Then σ_z^2 is sum of each of the noise components σ_o^2 and is given by

$$\sigma_z^2 = 4\sigma_o^2 = N_o E_s . \tag{4.27}$$

Using Equations (4.24) and (4.27) in Equation (4.23), we get

$$\begin{aligned} P_e &= Q\left(\frac{4E_s}{\sqrt{N_o E_s}}\right) \\ &= Q\left(\sqrt{\frac{16E_s}{N_o}}\right). \end{aligned} \tag{4.28}$$

Substituting the energy per bit defined in Equation (4.11) into Equation (4.28), we obtain

$$\begin{aligned} P_e &= Q\left(\sqrt{\frac{8E_b}{N_o}}\right) \\ &= Q\left(2\sqrt{\frac{2E_b}{N_o}}\right). \end{aligned} \tag{4.29}$$

The probability of bit error P_b for a baseband equivalent SISO BPSK system is given by [9,10]

$$P_b = Q\left(\frac{\bar{Z}^+}{\sigma_z}\right). \tag{4.30}$$

In this case $\bar{Z}^+$ is given by

$$\bar{Z}^+ = E_b , \tag{4.31}$$

and

$$\sigma_z^2 = \frac{N_o E_b}{2} . \tag{4.32}$$

Thus, P_b is

$$P_b = Q\left(\sqrt{\frac{2E_b}{N_o}}\right). \tag{4.33}$$

A comparison of Equations (4.29) and (4.33) reveals an improvement in bit error performance in the MIMO system by a factor of two over the SISO system. For equal performance, this equates to a 3-dB gain.

3. Performance Simulation Results

The simulation was conducted with increasing E_s/N_o. The period T was set to 0.0001 seconds. The simulation run time was set at 500.0 seconds. Thus, the total number of bits in a single simulation run was five million bits.

The simulated probability of bit error for the MIMO system is plotted in Figure 14. The results are plotted with the theoretical results obtained in Equation (4.29). In addition, the theoretical probability of bit error for a baseband equivalent SISO system is plotted for comparison(Equation (4.33)). The simulated results follow the theoretical results very well.

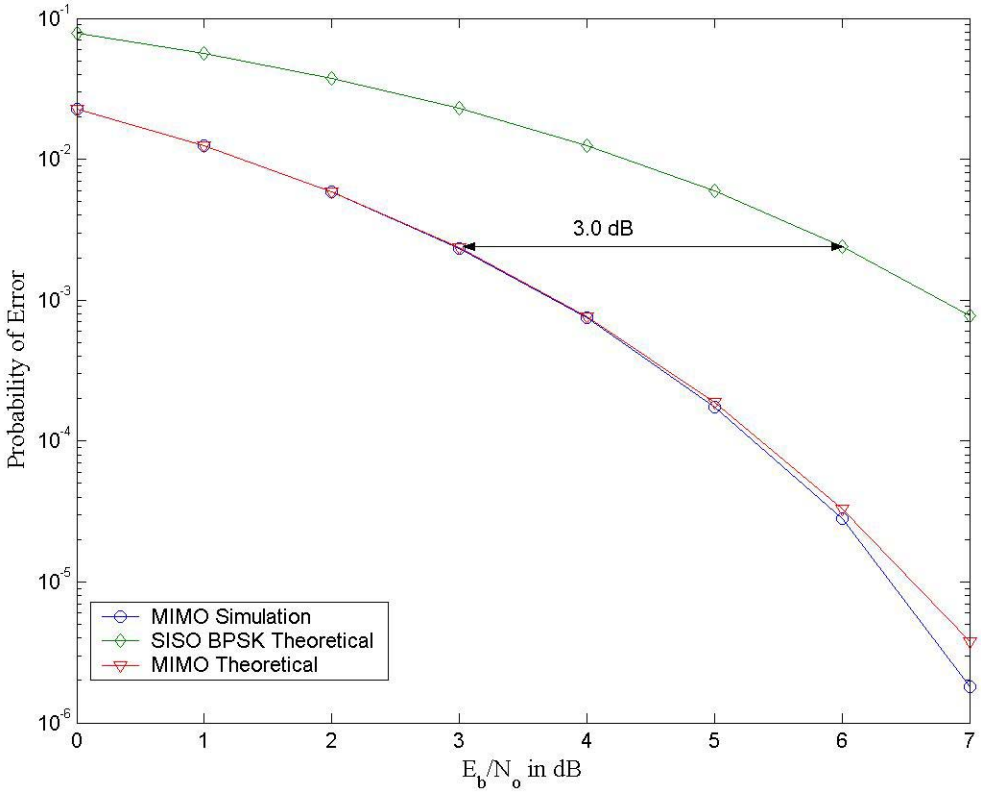

Figure 14. Results in AWGN.

They deviate starting at approximately 5.0 dB and above, but only by approximately 0.25 dB. This is a result of the number of bits in a single simulation run. If more bits are sent for comparison in a single simulation run, then comparison of simulated results with the theoretical results improves. This was confirmed with several experiments.

Nevertheless, overall the simulation of the MIMO system with five million bits follows the theoretical analysis of bit error performance very well.

C. SIMULATION IN A MULITPATH FADING CHANNEL

Next, the effect of the multipath fading channels are added. The simulation block diagram is given in Figure 15. A multipath fading channel is inserted for each independent path from transmitter to receive antenna. There are a total of four independent paths, each with a channel coefficient represented by h_{ij}.

1. Simulation Parameters

The multipath fading model was derived in Chapter II. Each multipath fading model is identical with respect to configuration. A block diagram is given in Figure 16. The model is the complex sum of two IID Gaussian random noise sources with zero-mean and equal variance. To distinguish these Gaussian random noise sources from the AWGN, they will be called Gaussian channel fade noise sources. The three parameters of the Gaussian channel fade noise sources that must be determined and controlled are the variance, the sample time and the initial seed. The initial seed determines the independence of the channel. Each of the seeds within the model is different. In this thesis the focus is on the case of all channel coefficients being statistically independent. Therefore, each of the initial seeds of all the other models is different. Consequently, there are eight different seeds for the Gaussian channel fade noise sources.

Next is the sample time. The sample time is determined such that the channel coefficients remain constant over the code sequence. Thus, the channel is slowly fading over the code sequence. The duration of the code sequence is $2T$ seconds, thus the sample time is set to $2T$ seconds.

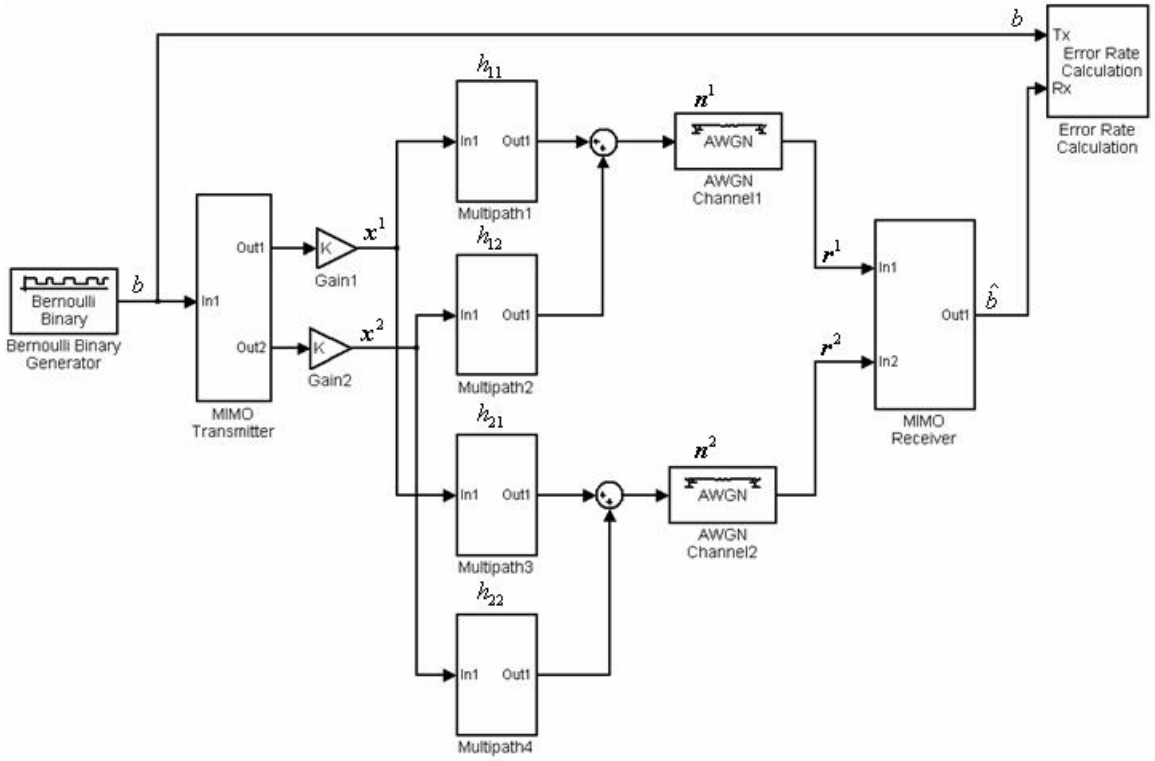

Figure 15. MIMO in multipath.

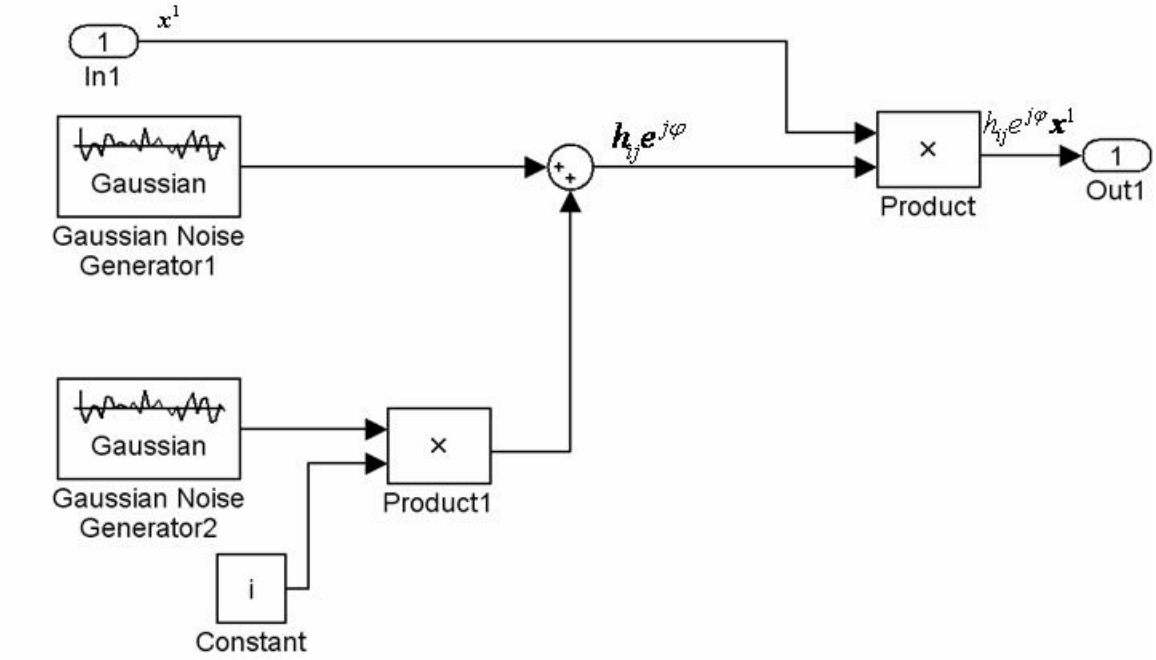

Figure 16. Fading model.

Lastly, the variance of the Gaussian channel fade noise sources is set to a value such that the total average signal power entering both AWGN blocks is 1.0 Watt. To determine the variance of the noise source, the energy per symbol at the output of Multipath1 is examined. Let the energy per symbol at the output of the fading channel be represented by E_h given by [9,10]

$$\begin{aligned} E_h &= \int_0^T \left| \frac{h_{11} A}{\sqrt{2}} \right|^2 dt \\ &= \frac{\left| h_{11} \right|^2 A^2 T}{2}. \end{aligned} \tag{4.34}$$

The channel coefficient is a random variable, so the average energy per symbol after the multipath channel is the mean of E_h. This can be obtained by taking the expected value of Equation (4.34) [5]. Then $\overline{E}_h$ is

$$\begin{aligned} \overline{E}_h &= \mathrm{E}\left[\frac{\left| h_{11} \right|^2 A^2 T}{2} \right] \\ &= \frac{A^2 T}{2} \mathrm{E}\left[h_{11}^2 \right]. \end{aligned} \tag{4.35}$$

The expected value of $\left| h_{11} \right|^2$ is the second moment of the Rayleigh distribution. The second moment can be determined from the mean and variance of the Rayleigh distribution defined in Chapter II by

$$\begin{aligned} \mathrm{E}\left[h_{11}^2 \right] &= \sigma_h^2 + \overline{h}^2 \\ &= \sigma^2 \left(2 - \frac{\pi}{2} \right) + \left(\sigma \sqrt{\frac{\pi}{2}} \right)^2 \\ &= 2\sigma^2. \end{aligned} \tag{4.36}$$

Note that σ^2 represents the variance of the Gaussian channel fade noise sources. Using Equation (4.36) in Equation (4.35), we obtain the average energy per symbol

$$\overline{E}_h = \sigma^2 A^2 T. \tag{4.37}$$

The average power per symbol $\overline{P}$ is

$$\overline{P} = \frac{\overline{E}_h}{T} = \sigma^2 A^2 . \tag{4.38}$$

The signal power at the input to either of the two AWGN channel blocks is the sum power of two multipath channel blocks. Each of the channel blocks has equal average signal power. Then the total average signal power $\overline{P}_t$ at either of the two AWGN blocks is

$$\overline{P}_t = 2\overline{P} = 2\sigma^2 A^2 . \tag{4.39}$$

The total average signal power $\overline{P}_t$ must equal 1.0 Watt. The amplitude A is equal to 1 Volt. Using this information in Equation (4.39), we find

$$\begin{aligned} 1 &= 2\sigma^2 \\ \sigma^2 &= \frac{1}{2}. \end{aligned} \tag{4.40}$$

Thus, the variances of all the Gaussian noises sources of the multipath fading channels are set to $1/2$.

2. Performance Analysis

With the addition of the multipath fading channels, at each receive antenna the received signals are

$$\begin{aligned} \boldsymbol{r}^1 &= \left(h_{11}\boldsymbol{x}^1 + h_{12}\boldsymbol{x}^2 \right) + \boldsymbol{n}^1 \\ \boldsymbol{r}^2 &= \left(h_{21}\boldsymbol{x}^1 + h_{22}\boldsymbol{x}^2 \right) + \boldsymbol{n}^2 . \end{aligned} \tag{4.41}$$

Once again, incorporating the definitions for $\boldsymbol{x^1}$ and $\boldsymbol{x^2}$ from Chapter III, Equation (4.41) becomes

$$\begin{aligned} \boldsymbol{r}^1 &= \left(h_{11}\left[x_1, -x_2^* \right] + h_{12}\left[x_2, x_1^* \right] \right) + \left[n_1^1, n_2^1 \right] \\ \boldsymbol{r}^2 &= \left(h_{21}\left[x_1, -x_2^* \right] + h_{22}\left[x_2, x_1^* \right] \right) + \left[n_1^2, n_2^2 \right]. \end{aligned} \tag{4.42}$$

The channel coefficients do not change over the code sequence and the noise acts on one symbol period. After serial-to-parallel conversion, the signals in each space diversity reception and time interval are given by

$$\boldsymbol{r}^1 = \left[r_1^1, r_2^1 \right] = \left[h_{11}x_1 + h_{12}x_2 + n_1^1, h_{12}x_1^* - h_{11}x_2^* + n_2^1 \right], \tag{4.43}$$

and

$$\boldsymbol{r}^2 = \left[r_1^2, r_2^2 \right] = \left[h_{21}x_1 + h_{22}x_2 + n_1^2, h_{22}x_1^* - h_{21}x_2^* + n_2^2 \right]. \tag{4.44}$$

After time diversity combination of the received signal on antenna 1, z_1^1 is

$$\begin{aligned} z_1^1 &= r_1^1 + \left(r_2^1 \right)^* \\ &= h_{11}x_1 + h_{12}x_2 + n_1^1 + \left(h_{12}x_1^* - h_{11}x_2^* + n_2^1 \right)^* \\ &= \left(h_{11} + h_{12}^* \right) x_1 + \left(h_{12} - h_{11}^* \right) x_2 + n_1^1 + n_2^{1*}, \end{aligned} \tag{4.45}$$

and z_2^1 is

$$\begin{aligned} z_2^1 &= r_1^1 - \left(r_2^1 \right)^* \\ &= h_{11}x_1 + h_{12}x_2 + n_1^1 - \left(h_{12}x_1^* - h_{11}x_2^* + n_2^1 \right)^* \\ &= \left(h_{11} - h_{12}^* \right) x_1 + \left(h_{12} + h_{11}^* \right) x_2 + n_1^1 - n_2^{1*}. \end{aligned} \tag{4.46}$$

Similarly, the time diversity combination of the received signal on antenna 2 for x_1 and x_2, represented by z_1^2 and z_2^2, respectively, are

$$\begin{aligned} z_1^2 &= \left(h_{21} + h_{22}^* \right) x_1 + \left(h_{22} - h_{21}^* \right) x_2 + n_1^2 + n_2^{2*} \\ z_2^2 &= \left(h_{21} - h_{22}^* \right) x_1 + \left(h_{22} + h_{21}^* \right) x_2 + n_1^2 - n_2^{2*}. \end{aligned} \tag{4.47}$$

After space diversity combining, z_1 is

$$\begin{aligned} z_1 &= z_1^1 + z_1^2 \\ &= \left(h_{11} + h_{12}^* + h_{21} + h_{22}^* \right) x_1 + \left(h_{12} - h_{11}^* + h_{22} - h_{21}^* \right) x_2 + n_1^1 + n_2^{1*} + n_1^2 + n_2^{2*}, \end{aligned} \tag{4.48}$$

and z_2 is

$$\begin{aligned} z_2 &= z_2^1 + z_2^2 \\ &= \left(\left(h_{11} - h_{12}^* + h_{21} - h_{22}^*\right)x_1 + \left(h_{12} + h_{11}^* + h_{22} + h_{21}^*\right)x_2\right) + n_1^1 - n_2^{1*} + n_1^2 - n_2^{2*}. \end{aligned} \tag{4.49}$$

Invoking the symmetry of receiver, we obtain the overall probability of error P_e by using z_1. The demodulator effectively takes the real part of z_1. Once again, let z be the real part of z_1. Then z is

$$\begin{aligned} z &= \mathrm{Re}\left[z_1\right] \\ &= \left(\mathrm{Re}\left[h_{11}\right] + \mathrm{Re}\left[h_{12}^*\right] + \mathrm{Re}\left[h_{21}\right] + \mathrm{Re}\left[h_{22}^*\right]\right)\mathrm{Re}\left[x_1\right] \\ &\quad + \left(\mathrm{Re}\left[h_{12}\right] - \mathrm{Re}\left[h_{11}^*\right] + \mathrm{Re}\left[h_{22}\right] - \mathrm{Re}\left[h_{21}^*\right]\right)\mathrm{Re}\left[x_2\right] \\ &\quad + \mathrm{Re}\left[n_1^1\right] + \mathrm{Re}\left[n_2^{1*}\right] + \mathrm{Re}\left[n_1^2\right] + \mathrm{Re}\left[n_2^{2*}\right]. \end{aligned} \tag{4.50}$$

The real parts of any h_{ij} are IID, Gaussian random variables with zero-mean and equal variance. Their sum is also a Gaussian random variable with mean of zero and variance equal to the sum of the variances [5]. As already discussed, the real parts of the AWGN components are IID zero-mean with equal variance. Their sum is also a Gaussian random variable with zero-mean and variance equal to the sum of the variances. Let the sum of channel coefficients multiplied with x_1 be h_a. Let the sum of the channel coefficients multiplied with x_2 be h_b. Let the sum of the noise components be represented by n. The real parts of x_1 and x_2 are equal to x_1 and x_2. Equation (4.50) becomes

$$z = h_a x_1 + h_b x_2 + n. \tag{4.51}$$

The overall probability of bit error, P_e, can be determined by taking the sum of probability of error over all combinations of x_1 and x_2 [5]. If $A' = A/\sqrt{2}$, then the real part of x_1 and x_2 over all combinations of b_1 and b_2 are

$$\begin{array}{cccc} b_1 & b_2 & x_1 & x_2 \\ 0 & 0 & A' & A' \\ 0 & 1 & A' & -A' \\ 1 & 0 & -A' & A' \\ 1 & 1 & -A' & -A'. \end{array} \tag{4.52}$$

Now P_e is given by

$$\begin{aligned} P_e = &\Pr\{\text{error} \mid b_1 b_2 = 00\} \Pr\{b_1 b_2 = 00\} \\ &+ \Pr\{\text{error} \mid b_1 b_2 = 01\} \Pr\{b_1 b_2 = 01\} \\ &+ \Pr\{\text{error} \mid b_1 b_2 = 10\} \Pr\{b_1 b_2 = 10\} \\ &+ \Pr\{\text{error} \mid b_1 b_2 = 11\} \Pr\{b_1 b_2 = 11\} \end{aligned} \tag{4.53}$$

The probability b_1 and b_2 being a bit zero or one are equally likely; therefore, $\Pr(b_1 b_2 = 00) = \Pr(b_1 b_2 = 01) = \Pr(b_1 b_2 = 10) = \Pr(b_1 b_2 = 11) = 1/4$ and Equation (4.53) reduces to

$$\begin{aligned} P_e = \frac{1}{4}(&\Pr\{\text{error} \mid b_1 b_2 = 00\} + \Pr\{\text{error} \mid b_1 b_2 = 01\} \\ &+ \Pr\{\text{error} \mid b_1 b_2 = 10\} + \Pr\{\text{error} \mid b_1 b_2 = 11\}) \end{aligned} \tag{4.54}$$

In terms of X_1 and X_2, Equation (4.54) becomes

$$\begin{aligned} P_e = \frac{1}{4}(&\Pr[Z < 0 \mid X_1 = X_2 = A'] + \Pr[Z < 0 \mid X_1 = A', X_2 = -A'] \\ &+ \Pr[Z > 0 \mid X_1 = -A', X_2 = A'] + \Pr[Z > 0 \mid X_1 = X_2 = -A']). \end{aligned} \tag{4.55}$$

Concentrating on the first term of Equation (4.55) and incorporating this information in Equation (4.51), we get

$$z = h_a A' + h_b A' + n\,. \tag{4.56}$$

Equation (4.56) represents a linear transformation of three independent Gaussian random variables h_a, h_b and n. The linear transformation of Gaussian random variables remains Gaussian [5]. Therefore, z is a Gaussian random variable with mean equal to the sum of the means and variance equal to the sum of the variances. Each of h_a, h_b and

n have zero-means. Thus, z has a zero-mean. The first term of Equation (4.55) is given by [5]

$$\Pr\left[Z<0, X_1 = X_2 = A'\right] = \Pr\left[h_a A' + h_b A' + n < 0\right] = \frac{1}{2}. \tag{4.57}$$

Each of the three remaining terms in Equation (4.55) gives the same result; thus, the overall probability of bit error is

$$P_e = \frac{1}{4}\left[\frac{1}{2}+\frac{1}{2}+\frac{1}{2}+\frac{1}{2}\right] = \frac{1}{2}. \tag{4.58}$$

Therefore, the probability of bit error, P_e, for the system is 0.5, regardless of the of the signal or the power of the noise. This was confirmed by simulation for increasing average symbol energy to noise ratio E_s/N_o.

3. Performance Simulation Results

The simulation was conducted with increasing E_s/N_o. The period T was set to 0.001 seconds. The simulation run time was set at 100.0 seconds. Thus, the total number of bits in a single simulation run were 100,000.

The simulated probability of error for the MIMO system is plotted in Figure 17. The results are plotted with the theoretical results obtained in Equation (4.58) In addition, the theoretical probability of error for a baseband equivalent SISO BPSK system in a multipath channel derived in Chapter II is plotted for comparison. This is given by

$$\overline{P_e} = \left[\frac{1}{2}\left(1-\sqrt{\frac{\overline{\gamma}_l}{1+\overline{\gamma}_l}}\right)\right], \tag{4.59}$$

where $\overline{\gamma}_l$ is given by

$$\overline{\gamma}_l = \frac{E_b 2\sigma^2}{N_o}. \tag{4.60}$$

Recall from Equation (4.40) that $\sigma^2 = 1/2$ thus, Equation (4.60) becomes

$$\overline{\gamma}_l = \frac{E_b}{N_o}. \tag{4.61}$$

The simulated results follow the theoretical results very well. However, they do not give the performance expected by a baseband equivalent SISO BPSK in a multipath channel.

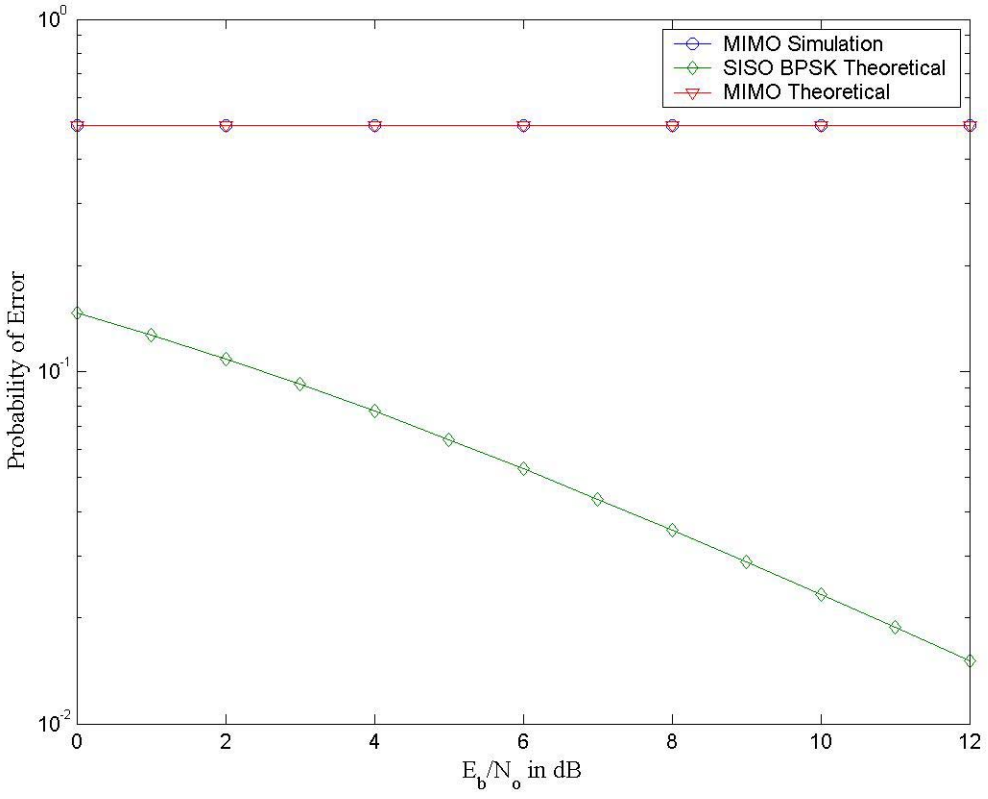

Figure 17. Results in Multipath Fading Channel.

The conclusion, of course, is that the receiver as designed in Chapter III and simulated in Figure 12 cannot communicate in a multipath fading channel. Thus, improvement to the receiver design must be incorporated in order for the system to function in a multipath channel. In the next section, the required improvement is incorporated in the design: the MRC receiver with CSI.

D. SIMULATION IN A MULTIPATH CHANNEL WITH MRC DESIGN

An MRC receiver incorporates CSI [10]. The incorporation of CSI follows that found in Reference [13]. Nevertheless, before discussing the design of the receiver, the received signals are examined more closely. Investigation of Equations (4.43) and (4.44) once again gives

$$\begin{aligned} r_1^1 &= h_{11}x_1 + h_{12}x_2 + n_1^1 \\ r_2^1 &= h_{12}x_1^* - h_{11}x_2^* + n_2^1 \\ r_1^2 &= h_{21}x_1 + h_{22}x_2 + n_1^2 \\ r_2^2 &= h_{22}x_1^* - h_{21}x_2^* + n_2^2. \end{aligned} \tag{4.62}$$

Next, we take the complex conjugate of r_2^1 and r_2^2, and Equation (4.62) becomes

$$\begin{aligned} r_1^1 &= h_{11}x_1 + h_{12}x_2 + n_1^1 \\ \left(r_2^1\right)^* &= h_{12}^*x_1 - h_{11}^*x_2 + n_2^{1*} \\ r_1^2 &= h_{21}x_1 + h_{22}x_2 + n_1^2 \\ \left(r_2^2\right)^* &= h_{22}^*x_1 - h_{21}^*x_2 + n_2^{2*}. \end{aligned} \tag{4.63}$$

We would be well served to view Equation (4.63) as describing a 2-input, 4-output MIMO system. This equation set can be represented in matrix form as

$$\mathbf{r} = \mathbf{H}\mathbf{x} + \mathbf{n}, \tag{4.64}$$

where $\mathbf{r}$ is

$$\mathbf{r} = \begin{bmatrix} r_1^1 \\ r_1^2 \\ \left(r_2^1\right)^* \\ \left(r_2^2\right)^* \end{bmatrix}, \tag{4.65}$$

$\mathbf{x}$ is

$$\mathbf{x} = \begin{bmatrix} x_1 \\ x_2 \end{bmatrix}, \tag{4.66}$$

$\mathbf{H}$ is

$$\mathbf{H} = \begin{bmatrix} h_{11} & h_{12} \\ h_{21} & h_{22} \\ h_{12}^* & -h_{11}^* \\ h_{22}^* & -h_{21}^* \end{bmatrix}, \tag{4.67}$$

and $\mathbf{n}$ is

$$\mathbf{n} = \begin{bmatrix} n_1^1 \\ n_1^2 \\ n_2^{1*} \\ n_2^{2*} \end{bmatrix}. \tag{4.68}$$

Note that the second and third lines in Equation (4.63) were swapped in the definitions described in Equations (4.66), (4.67) and (4.68).

From Chapter II and Reference [1], the capacity is dependent on matrix $\mathbf{Q}$ given in Equation (2.74) by

$$\mathbf{Q} = \mathbf{H}^{*T}\mathbf{H}. \tag{4.69}$$

Using the definition of $\mathbf{H}$ in Equation (4.67), we get

$$\begin{aligned} \mathbf{Q} &= \mathbf{H}^{*T}\mathbf{H} \\ &= \begin{bmatrix} h_{11}^* & h_{21}^* & h_{12} & h_{22} \\ h_{12}^* & h_{22}^* & -h_{11} & -h_{21} \end{bmatrix} \begin{bmatrix} h_{11} & h_{12} \\ h_{21} & h_{22} \\ h_{12}^* & -h_{11}^* \\ h_{22}^* & -h_{21}^* \end{bmatrix}, \end{aligned} \tag{4.70}$$

which reduces to

$$\mathbf{Q} = \begin{bmatrix} \left(|h_{11}|^2 + |h_{12}^2|^2 + |h_{21}|^2 + |h_{22}|^2 \right) & 0 \\ 0 & \left(|h_{11}|^2 + |h_{12}|^2 + |h_{21}|^2 + |h_{22}|^2 \right) \end{bmatrix}. \tag{4.71}$$

As discussed in Chapter II and Reference [1], this is a form of matrix $\mathbf{Q}$ that gives a linear increase in capacity with size of $\mathbf{Q}$, in this case two. If CSI is used appropriately, then this capacity can be approached. In the receiver, if channel

priately, then this capacity can be approached. In the receiver, if channel information is used according to $\mathbf{H}^{*T}$, then this can be achieved.

It seems extraordinary that the matrix $\mathbf{H}$ has this property. However, it was the code and the reception of the code that forced this property [13]. Referring to Chapter III, we see that the code matrix $\mathbf{X}$ had this same property. Thus, in receiving this code, the channel matrix $\mathbf{H}$ has this property regardless of h_{ij}, the channel realization over the code interval [13].

The use of CSI must be incorporated according to $\mathbf{H}^{*T}$. Given the received matrix $\mathbf{r}$, let a signal matrix $\mathbf{z}$ be defined by

$$\mathbf{z} = \mathbf{H}^{*T}\mathbf{r}. \tag{4.72}$$

This is consistent with Reference [13]. Thus, the implementation of CSI is accomplished according to Equation (4.72).

The expansion of Equation (4.72) gives

$$\begin{aligned}\mathbf{z} &= \begin{bmatrix} h_{11}^* & h_{21}^* & h_{12} & h_{22} \\ h_{12}^* & h_{22}^* & -h_{11} & -h_{21} \end{bmatrix} \begin{bmatrix} r_1^1 \\ r_1^2 \\ \left(r_2^1\right)^* \\ \left(r_2^2\right)^* \end{bmatrix} \\ &= \begin{bmatrix} h_{11}^* r_1^1 + h_{21}^* r_1^2 + h_{12}\left(r_2^1\right)^* + h_{22}\left(r_2^2\right)^* \\ h_{12}^* r_1^1 + h_{22}^* r_1^2 - h_{11}\left(r_2^1\right)^* - h_{21}\left(r_2^2\right)^* \end{bmatrix}. \end{aligned} \tag{4.73}$$

1. Simulation Parameters

Equation (4.73) represents the rules for incorporating the CSI. The modified receiver that incorporates the use of CSI is described in Figure 18. The modified receiver is a MRC receiver. The simulation of the MRC receiver is described in Figure 19. The channel parameters h_{11}, h_{12}, h_{21} and h_{22} are taken directly from the appropriate multipath fading block. This provides perfect channel knowledge.

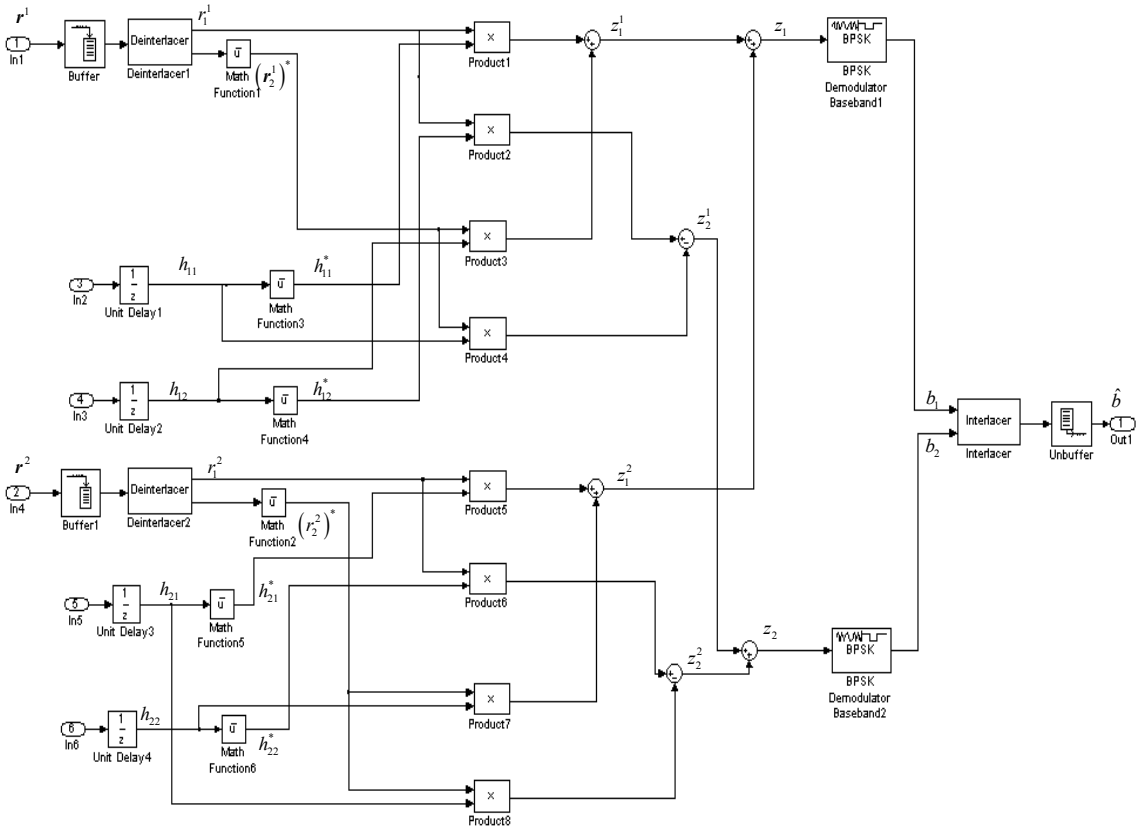

Figure 18. MIMO Receiver with CSI implementation.

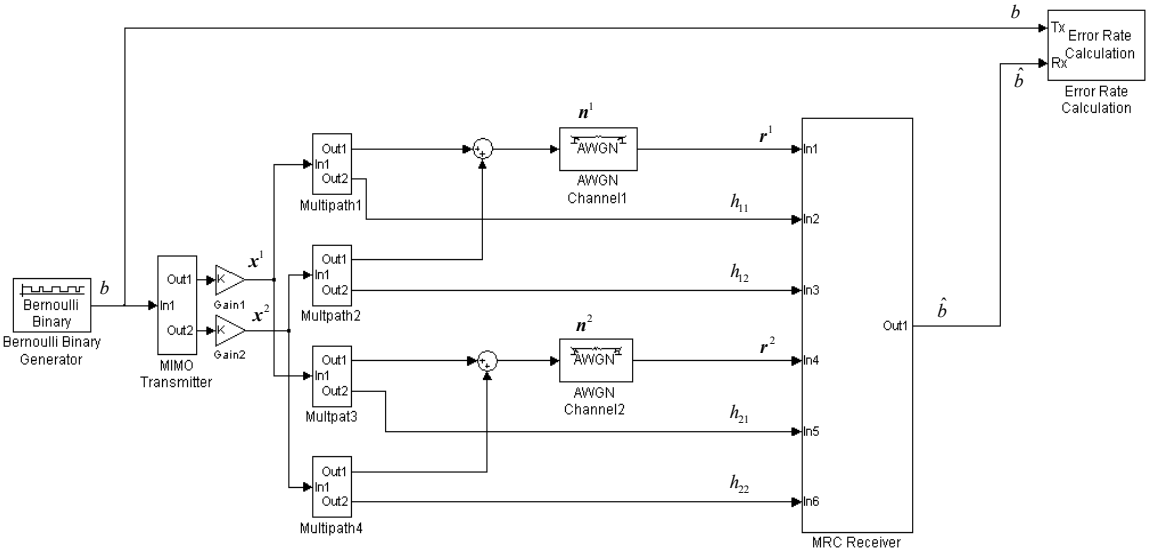

Figure 19. Multipath Simulation with MIMO MRC receiver.

In order to coincide with the correct symbols at the multipliers, the channel coefficients are delayed by $2T$ seconds since the buffers in the receiver induces this delay. The remainder of the simulation parameters remain the same as in previous simulations.

2. Performance Analysis

The received signal matrix $\mathbf{z}$ represents the signals z_1 and z_2 given by

$$\mathbf{z} = \begin{bmatrix} z_1 \\ z_2 \end{bmatrix} = \mathbf{H}^{*T}\mathbf{r}, \tag{4.74}$$

which expands to

$$\begin{aligned} \mathbf{z} &= \mathbf{H}^{*T}\mathbf{H}\mathbf{x} + \mathbf{H}^{*T}\mathbf{n} \\ \mathbf{z} &= \mathbf{Q}\mathbf{x} + \mathbf{H}^{*T}\mathbf{n}. \end{aligned} \tag{4.75}$$

After matrix multiplication, Equation (4.75) expands to

$$\mathbf{z} = \begin{bmatrix} z_1 \\ z_2 \end{bmatrix} = \begin{bmatrix} \left(|h_{11}|^2 + |h_{21}|^2 + |h_{12}|^2 + |h_{22}|^2\right)x_1 + h_{11}^* n_1^1 + h_{12} n_2^{1*} + h_{21}^* n_1^2 + h_{22} n_1^{2*} \\ \left(|h_{11}|^2 + |h_{21}|^2 + |h_{12}|^2 + |h_{22}|^2\right)x_2 - h_{11} n_2^1 + h_{12}^* n_1^1 - h_{21} n_2^{2*} + h_{22}^* n_1^1 \end{bmatrix}. \tag{4.76}$$

Applying the symmetry of the receiver, we only have to investigate z_1. The result of Equation (4.76) equates to an MRC receiver with $L = 4$ diversity receptions [10]. The probability of error of z_1 was given in Chapter II, that is,

$$\overline{P_e} = \left[\frac{(1-u)}{2}\right]^L \sum_{l=0}^{L-1} \binom{L-1+l}{l} \left[\frac{(1+u)}{2}\right]^l, \tag{4.77}$$

where u is

$$u = \sqrt{\frac{\overline{\gamma}_l}{1+\overline{\gamma}_l}}, \tag{4.78}$$

and $\overline{\gamma}_l$ is

$$\overline{\gamma}_l = \frac{E2\sigma^2}{N_0}. \tag{4.79}$$

The parameter E in Equation (4.79) represents the energy per symbol E_s. The energy per symbol is given by

$$E_s = \frac{E_b}{2}. \tag{4.80}$$

Since $\sigma^2 = 1/2$, Equation (4.79) becomes

$$\overline{\gamma}_l = \frac{E_b}{2N_0}. \tag{4.81}$$

3. Performance Simulation Results

The simulation was conducted with increasing E_s/N_o. As was the case in the AWGN simulation, the period, T, was set to 0.0001 seconds. The simulation run time was set at 500.0 seconds giving the total number bits in a single simulation run of five million.

The simulated probability of error for the MIMO systems is plotted in Figure 20. The results are plotted with the theoretical results given by Equations (4.77), (4.78) and (4.81). As well, the theoretical probability of error for a SISO BPSK system is plotted for comparison. Note that the SISO BPSK system has perfect knowledge of the CSI. The MIMO system's simulated results, with MRC receiver, follow the theoretical results very well. The simulated results deviate starting at approximately 13.0 dB. This is a result of the number of bits per simulation run. Overall, the simulation follows the theoretical analysis of bit error performance. Also indicated in the figure is the improvement in bit error performance over the single channel BPSK system. For equal E_b/N_o, there is an excellent improvement in performance that increases as E_b/N_o increases. This improvement follows the expected improvement as illustrated in Chapter II. Lastly, the system achieved $L = 4$ diversity order; specifically, the sum of two time diversity and two

space diversity orders. This is consistent with the potential of the Alamouti space–time code [1,13].

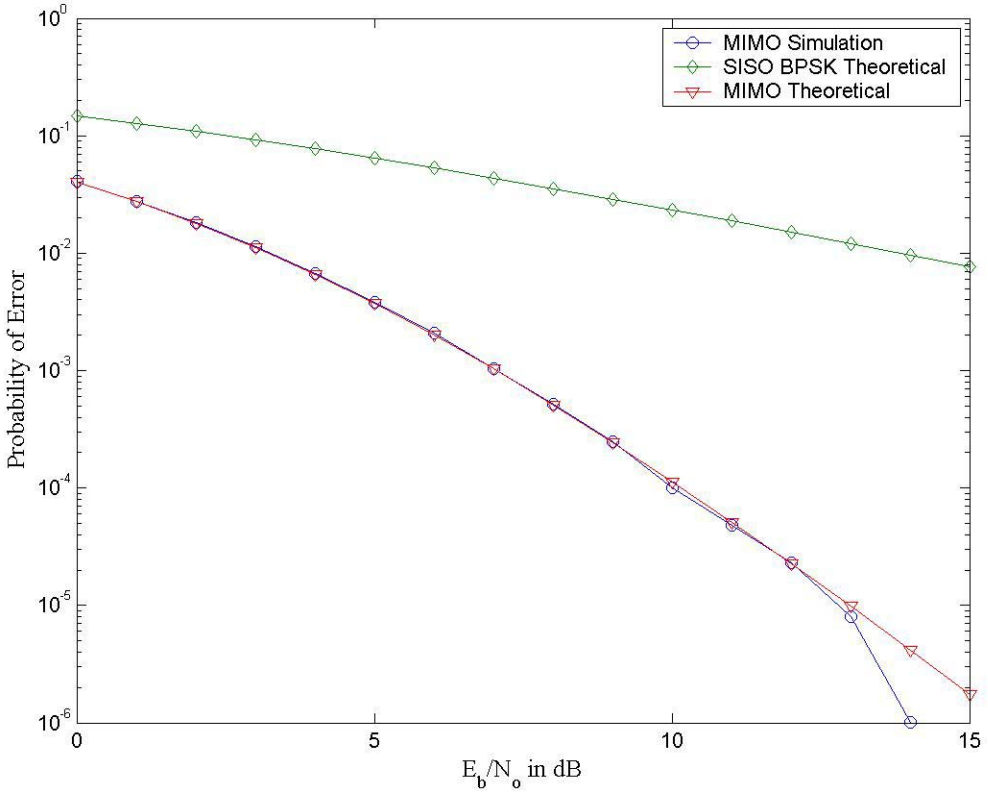

Figure 20. Results MRC Multipath fading.

Found in Reference [1] are the results for probability of error for a MIMO system using the Alamouti scheme. They are given in Figure 21. The published results follow the same assumptions, i.e., the channels are independent and perfect CSI is known [1]. In the figure, the graph with the circle markings is the one of primary interest, which corresponds to the simulation in this thesis. The graph indicates very similar results, particularly at $E_b / N_o = 10$ dB, where P_e is approximately 10^{-4}.

E. SUMMARY OF RESULTS

In this chapter, the MIMO system designed in Chapter III was examined with AWGN only as well as the effects of multipath. The MIMO system performed as ex-

pected with only AWGN and achieved better performance than a SISO BPSK system. The system was than simulated for a multipath channel. As designed, it was not able to communicate through this channel. The receiver for the original system was converted to an MRC receiver with CSI. As a result, the new design was able to communicate successfully in the multipath channel. The performance of the new design matched expected theoretical performance. Additionally, it also outperformed a SISO BPSK system.

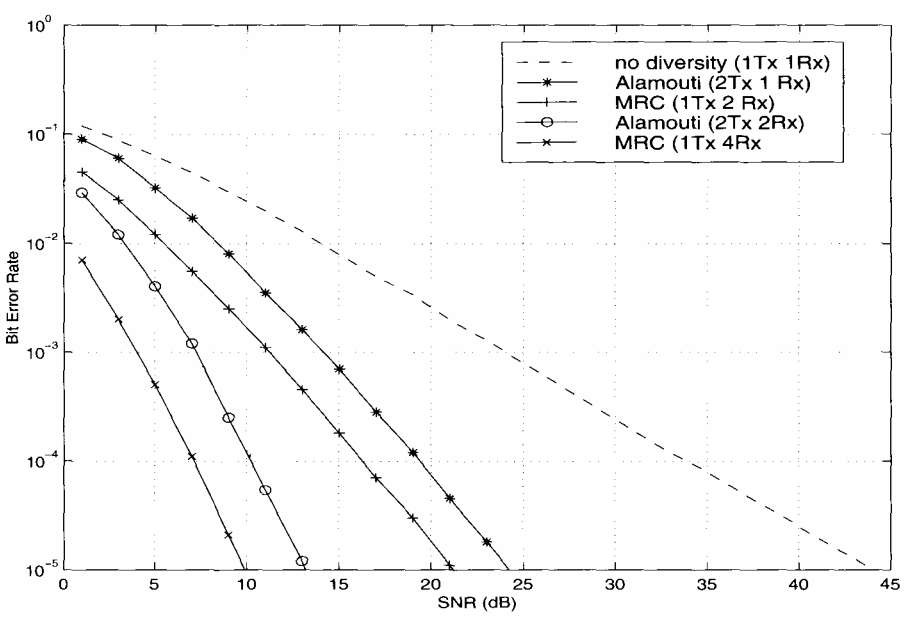

Figure 21. Published results (From Reference [1].).

Furthermore, the system's performance compared well with published results. The MIMO system was able to achieve $L = 4$ diversity order with the Alamouti space–time code, which is consistent with published results.

In the next chapter, the results of this thesis are summarized and areas for follow-on work are presented.

THIS PAGE INTENTIONALLY LEFT BLANK

V. CONCLUSION

The goal of this thesis was to develop a MIMO system with space–time coding with an eye towards military application. A MIMO system was designed using the Alamouti space–time code. It was simulated in Matlab with Simulink and was tested in a progressive manner, first in an AWGN channel and then in a multipath fading channel with AWGN. The performance of the system was analyzed and compared with simulated results, as well as published results found in Reference [1].

A. RESULTS

The designed MIMO system performed in a manner consistent with theoretical analysis in the AWGN channel. The simulated results compared very well with the theoretical performance analysis. However, the original design failed in a multipath channel with AWGN. The design did not incorporate CSI and a MRC receiver. Nevertheless, performance analysis was derived and simulated results reflected the anticipated theoretical results. With this failure, the original receiver design was changed to an MRC receiver incorporating CSI. Consequently, the new design was able to communicate successfully in the multipath channel. The performance of the new design matched expected theoretical performance, as well as published results. Finally, the designed MIMO system with the MRC receiver was able to achieve full diversity order with the Alamouti space–time code which was consistent with published results. There is improved bit error performance in the MIMO system over the SISO system and capacity gain which can be exploitable for military application.

B. FOLLOW-ON WORK

There are three areas identified for follow-on work. First, the designed MIMO receiver can be converted into a maximum–likelihood decoding receiver. This design holds promise of simplicity over the original design. The performance analysis can be investigated and simulated.

Next, higher order space–time codes can be investigated. Although the Alamouti space–time code can achieve full diversity gain, it is unable to achieve coding gain as discussed in Chapter II without bandwidth expansion. Higher order codes can be examined and tested by augmenting the original design or using a maximum–likelihood decoding receiver. The incorporation of ECC can be investigated in conjunction with the modulation scheme in order to achieve coding gain.

Lastly, the MIMO system is already using CSI at the receiver. If this information about the channel can be extracted at the receiver, then it can be sent to the transmitter. The transmitter can use CSI to more efficiently transmit power to the receiver through channels that are less faded than others. Techniques that control the transmitter can be investigated and performance of the system analyzed.

APPENDIX A. LIST OF ACRONYMS

AWGN	Additive White Gaussian Noise
BPSK	Binary Phase–Shift Keying
CSI	Channel State Information
ECC	Error Control Coding
IID	Independent Identically Distributed
MIMO	Multiple–Input–Multiple–Output
MRC	Maximal-ratio Combining
SISO	Single–Input–Single–Output
SNR	Signal-to-Noise Ratio
SVD	Singular Value Decomposition

THIS PAGE INTENTIONALLY LEFT BLANK

APPENDIX B. MATLAB SIMULINK BLOCK PARAMETERS

The block parameters shown in this appendix give the parameters and a brief description of the Matlab blocks used in the simulations in this thesis.

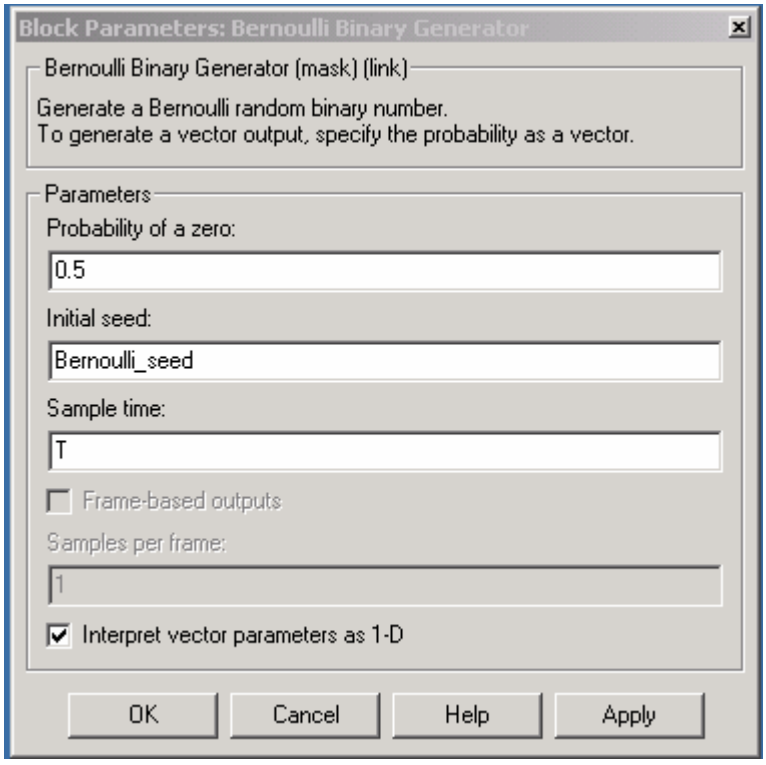

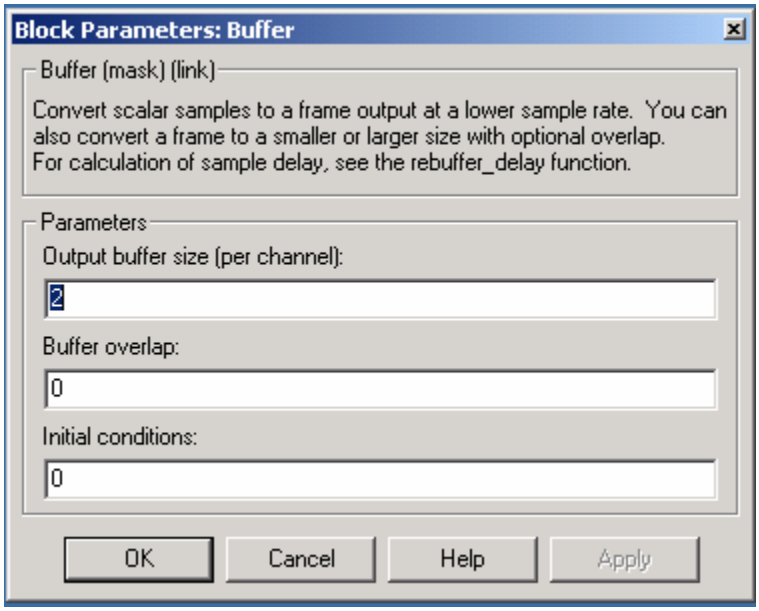
Block Parameters: Buffer
Buffer (mask) (link)
Convert scalar samples to a frame output at a lower sample rate. You can also convert a frame to a smaller or larger size with optional overlap.
For calculation of sample delay, see the rebuffer_delay function.
Parameters
Output buffer size (per channel):
2
Buffer overlap:
0
Initial conditions:
0
OK
Cancel
Help
Apply

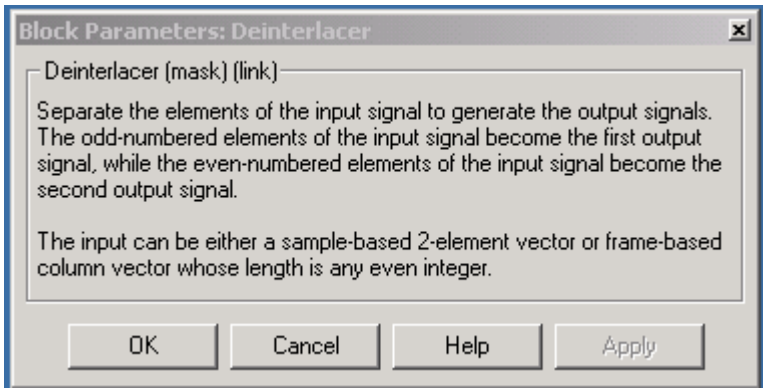
Block Parameters: Deinterlacer
Deinterlacer (mask) (link)
Separate the elements of the input signal to generate the output signals. The odd-numbered elements of the input signal become the first output signal, while the even-numbered elements of the input signal become the second output signal.
The input can be either a sample-based 2-element vector or frame-based column vector whose length is any even integer.
OK
Cancel
Help
Apply

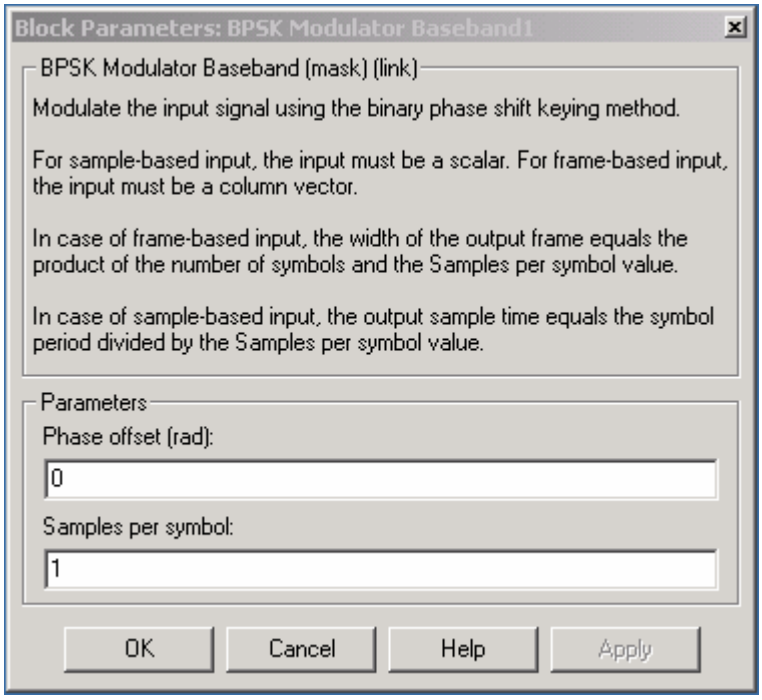
Block Parameters: BPSK Modulator Baseband1
BPSK Modulator Baseband (mask) (link)
Modulate the input signal using the binary phase shift keying method.
For sample-based input, the input must be a scalar. For frame-based input, the input must be a column vector.
In case of frame-based input, the width of the output frame equals the product of the number of symbols and the Samples per symbol value.
In case of sample-based input, the output sample time equals the symbol period divided by the Samples per symbol value.
Parameters
Phase offset (rad):
0
Samples per symbol:
1
OK
Cancel
Help
Apply

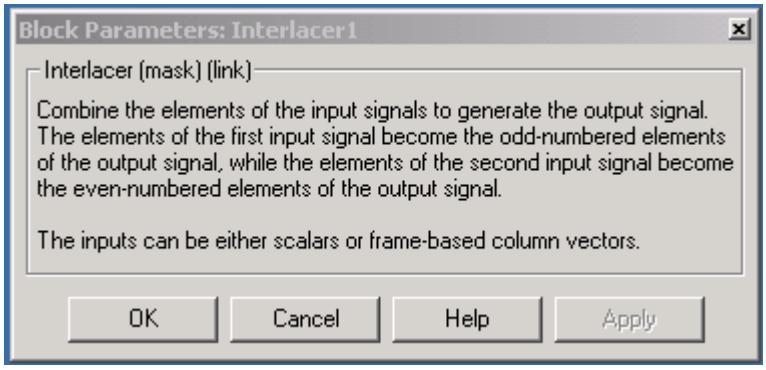
Block Parameters: Interlacer1
Interlacer (mask) (link)
Combine the elements of the input signals to generate the output signal. The elements of the first input signal become the odd-numbered elements of the output signal, while the elements of the second input signal become the even-numbered elements of the output signal.
The inputs can be either scalars or frame-based column vectors.
OK
Cancel
Help
Apply

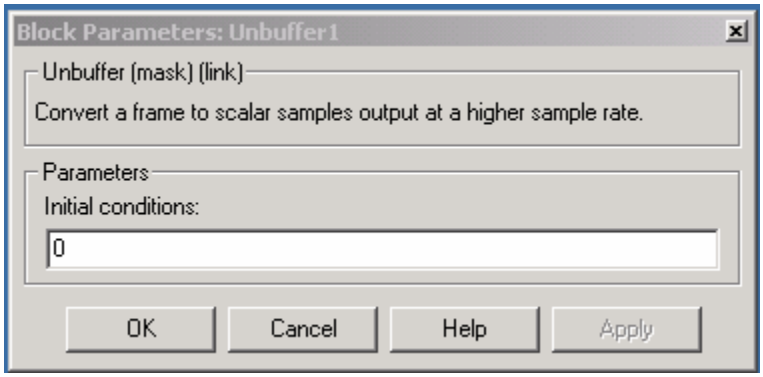
Block Parameters: Unbuffer1
Unbuffer (mask) (link)
Convert a frame to scalar samples output at a higher sample rate.
Parameters
Initial conditions:
0
OK
Cancel
Help
Apply

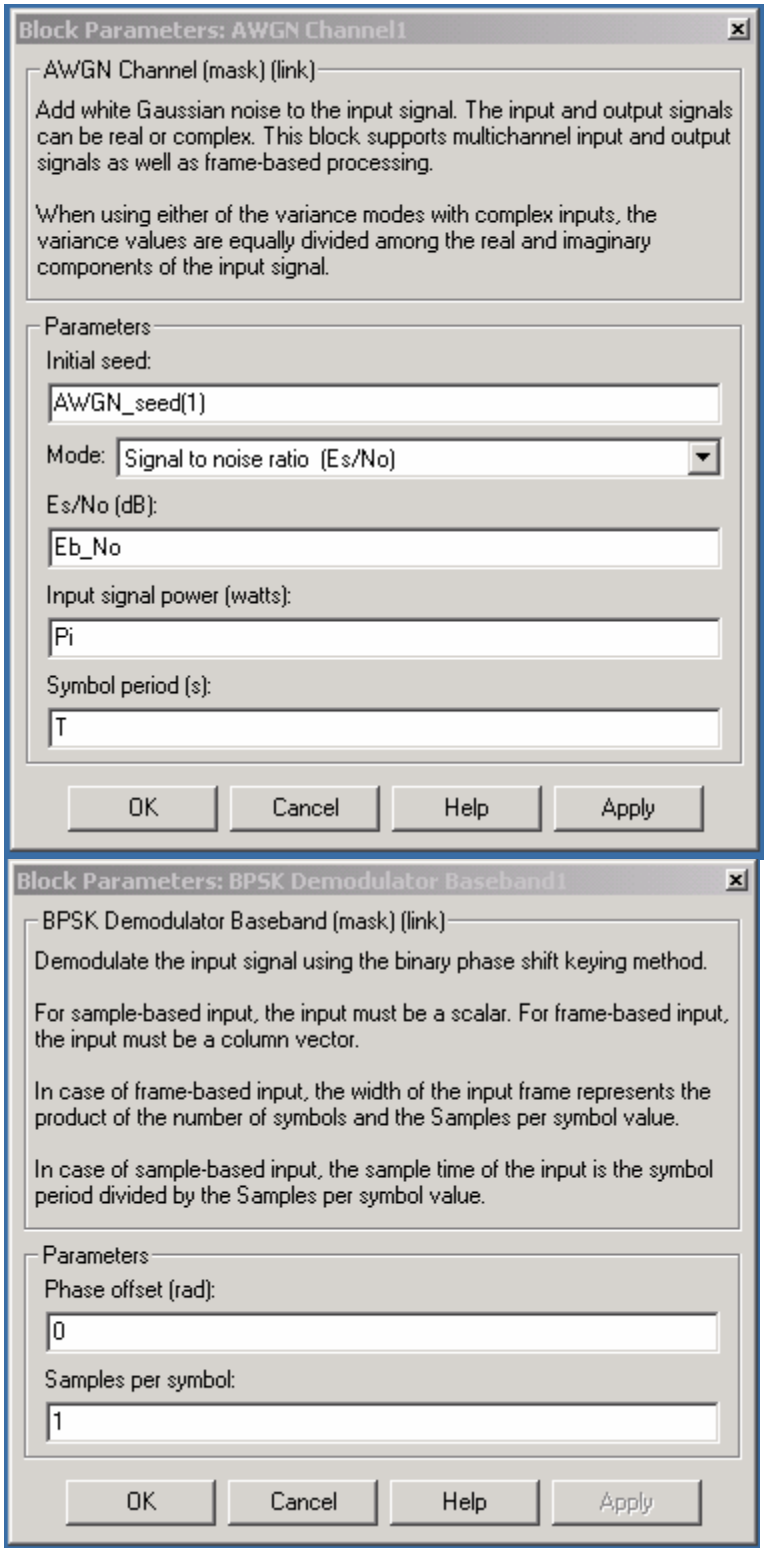
Block Parameters: AWGN Channel1
AWGN Channel (mask) (link)
Add white Gaussian noise to the input signal. The input and output signals can be real or complex. This block supports multichannel input and output signals as well as frame-based processing.
When using either of the variance modes with complex inputs, the variance values are equally divided among the real and imaginary components of the input signal.
Parameters
Initial seed:
AWGN_seed(1)
Mode: Signal to noise ratio (Es/No)
Es/No (dB):
Eb_No
Input signal power (watts):
Pi
Symbol period (s):
T
OK
Cancel
Help
Apply
Block Parameters: BPSK Demodulator Baseband1
BPSK Demodulator Baseband (mask) (link)
Demodulate the input signal using the binary phase shift keying method.
For sample-based input, the input must be a scalar. For frame-based input, the input must be a column vector.
In case of frame-based input, the width of the input frame represents the product of the number of symbols and the Samples per symbol value.
In case of sample-based input, the sample time of the input is the symbol period divided by the Samples per symbol value.
Parameters
Phase offset (rad):
0
Samples per symbol:
1
OK
Cancel
Help
Apply

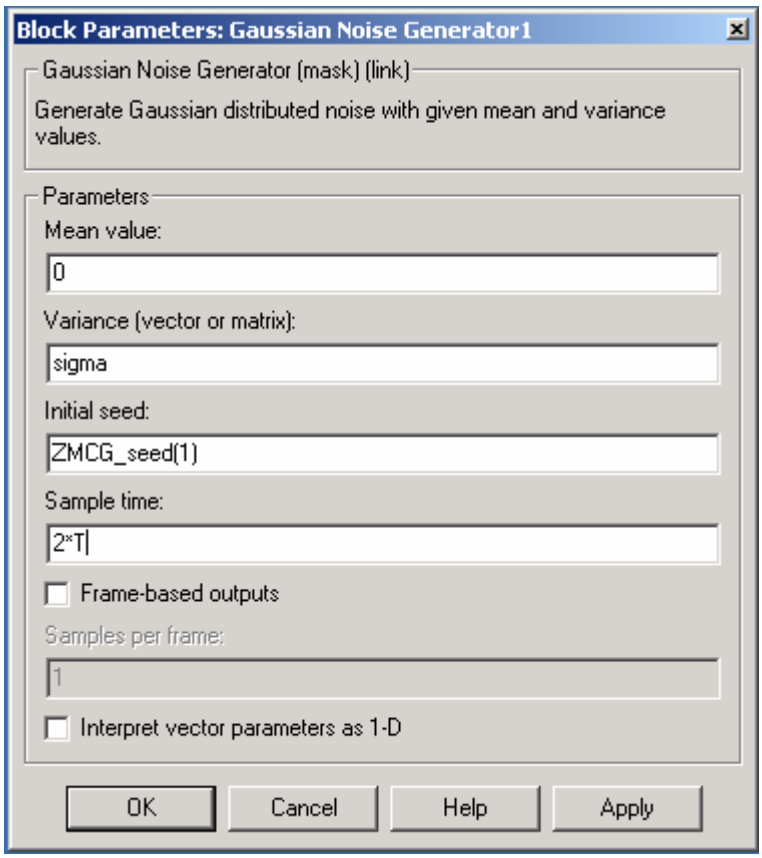
Block Parameters: Gaussian Noise Generator1
Gaussian Noise Generator (mask) (link)
Generate Gaussian distributed noise with given mean and variance values.
Parameters
Mean value:
0
Variance (vector or matrix):
sigma
Initial seed:
ZMCG_seed(1)
Sample time:
2*T
Frame-based outputs
Samples per frame:
1
Interpret vector parameters as 1-D
OK
Cancel
Help
Apply

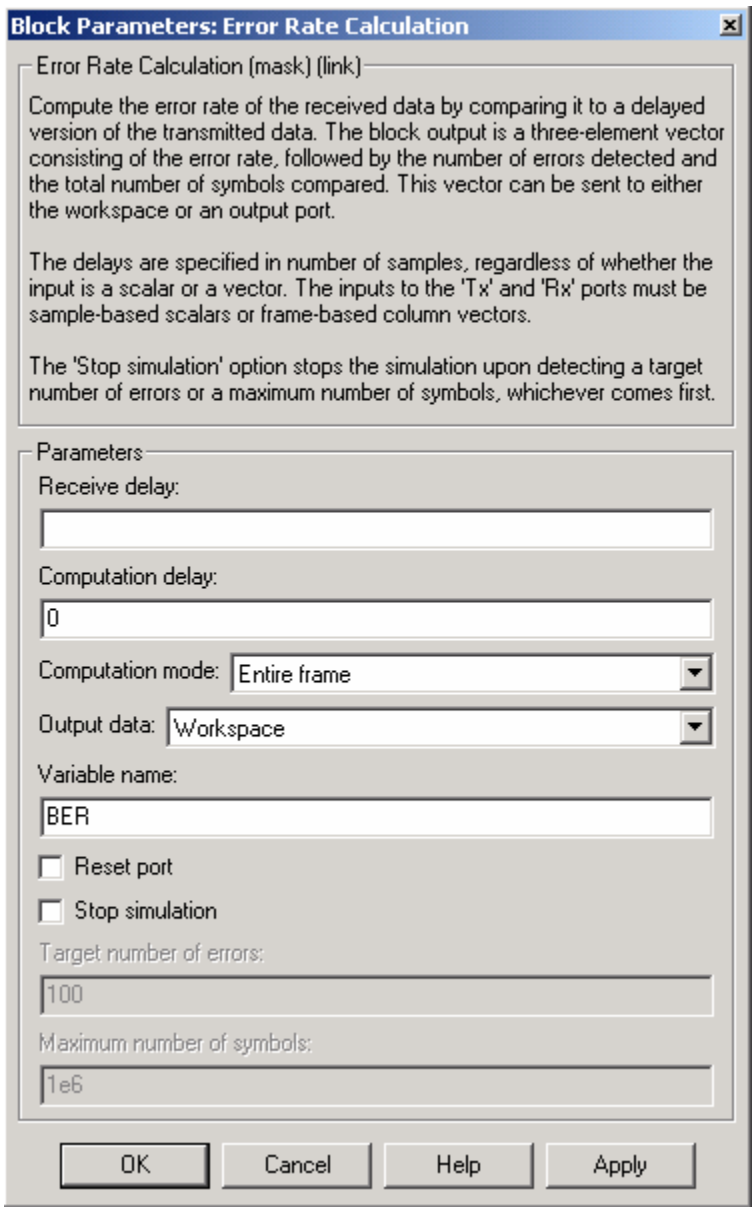
Block Parameters: Error Rate Calculation
Error Rate Calculation (mask) (link)
Compute the error rate of the received data by comparing it to a delayed version of the transmitted data. The block output is a three-element vector consisting of the error rate, followed by the number of errors detected and the total number of symbols compared. This vector can be sent to either the workspace or an output port.
The delays are specified in number of samples, regardless of whether the input is a scalar or a vector. The inputs to the 'Tx' and 'Rx' ports must be sample-based scalars or frame-based column vectors.
The 'Stop simulation' option stops the simulation upon detecting a target number of errors or a maximum number of symbols, whichever comes first.
Parameters
Receive delay:
Computation delay:
0
Computation mode:
Entire frame
Output data:
Workspace
Variable name:
BER
Reset port
Stop simulation
Target number of errors:
100
Maximum number of symbols:
1e6
OK
Cancel
Help
Apply

LIST OF REFERENCES

[1] Branka Vucetic and Jinhong Yuan, *Space-Time Coding*, John Wiley & Sons, West Sussex, England, 2003.

[2] M.A. Beach, D.P. McNamara, P.N. Fletcher and P. Karlsson, "MIMO — A solution for advanced wireless access?," *Proc. 11th International Conference on Antennas and Propagation*, pp. 231–235, IEEE Conference Publication No. 480, 2001.

[3] Simon Haykin, *An Introduction to Analog and Digital Communications,* John Wiley & Sons, New York, 1989.

[4] Charles W. Therrien, *Discrete Random Signals and Statistical Signal Processing,* Prentice Hall, Upper Saddle River, NJ, 1992.

[5] Peyton Z. Peebles Jr., *Probability, Random Variables and Random Signal Principles,* Fourth Edition, McGraw-Hill, New York, 2001.

[6] Erwin Kreyszig, *Advanced Engineering Mathematics,* Fourth Edition, John Wiley & Sons, New York, 1979.

[7] Bernard Sklar, *Digital Communications Fundamentals and Applications,* Second Edition, Prentice Hall, Upper Saddle River, NJ, 2002.

[8] Seymour Lipschutz, *Schaum's Outline of Theory and Problems of Linear Algebra*, McGraw-Hill, New York, 1968

[9] Clark Robertson, Notes EC4550 (M-Ary Digital Communications Systems), Naval Postgraduate School, Monterey, CA, 2004 (unpublished).

[10] John G. Proakis, *Digital Communications*, Fourth Edition, McGraw-Hill, New York, 2001.

[11] Theodore S. Rappaport, *Wireless Communications Principals and Practice*, Second Addition., Prentice-Hall PTR, Upper Saddle River, NJ 2002.

[12] Murali Tummala, Notes EC2010 (Probabilistic Analysis of Signals and Systems), Naval Postgraduate School, Monterey, CA, 2003 (unpublished).

[13] Arogyaswami Paulraj, Rohit Nabar and Dhananjay Gore, *Introduction to Space–Time Wireless Communications,* Cambridge University Press, New York, 2003.

[14] Siavash M. Alamouti, "A simple transmit diversity technique for wireless communications," *IEEE Journal on Select Areas in Communications*, vol. 16, no. 8, pp. 1451-1458, October 1998.

[15] *MATLAB Helpfile*, The MathWorks, Inc., Version 6.5.0.180913a Release 13, Natick, MA, 18 June 2002.

INITIAL DISTRIBUTION LIST

1. Defense Technical Information Center
   Ft. Belvoir, Virginia

2. Dudley Knox Library
   Naval Postgraduate School
   Monterey, California

3. Chairman, Code EC
   Electrical and Computer Engineering Department
   Naval Postgraduate School
   Monterey, California

4. Frank Kragh, Code/EC/kh
   Electrical and Computer Engineering Department
   Naval Postgraduate School
   Monterey, California

5. Clark Robertson, Code/EC/Rc
   Electrical and Computer Engineering Department
   Naval Postgraduate School
   Monterey, California

6. Michael Turpin
   Orleans ON, Canada